Hindawi
Journal of Food Biochemistry
Volume 2023, Article ID 8622745, 19 pages
https://doi.org/10.1155/2023/8622745

Research Article

Protective Effect of *Alpinia oxyphylla* Fructus Polysaccharides Extracted with Different Solvents on Dextran Sulfate Sodium-Induced Ulcerative Colitis in Mice

Xinyue Ma,[1] Liyan Li,[1] Dezhi Deng,[1] Yinfeng Tan,[1] Yuhuang Wu,[1] Guxu Ming,[1] Qiaoling Zhang,[1] Xiaoning He ,[2] and Yonghui Li [1,2]

[1]*Hainan Provincial Key Laboratory of R&D on Tropical Herbs, Haikou Key Laboratory of Li Nationality Medicine, School of Pharmacy, Hainan Medical University, Haikou 571199, China*
[2]*The Second Affiliated Hospital of Hainan Medical University, Haikou 571199, China*

Correspondence should be addressed to Xiaoning He; hexiaoningvv@aliyun.com and Yonghui Li; lyhssl@126.com

Received 23 May 2023; Revised 27 August 2023; Accepted 16 September 2023; Published 26 September 2023

Academic Editor: Kai Wang

Ulcerative colitis (UC) is a temporary incurable inflammatory bowel disease. *Alpinia oxyphylla* fructus polysaccharides (AOFPs) have anti-inflammatory, antioxidant, and other biological activities. In order to explore the therapeutic effect of AOFPs on UC, this study used deionized water, NaCl, HCl, and NaOH to extract AOFPs, and their protective effects on UC were evaluated by dextran sulfate sodium-induced UC mouse model. The results showed that extraction solvents had significant effects on the yield, molecular weights, monosaccharide compositions, total sugar contents, uronic acid contents, protein contents, and surface morphology of AOFPs. Histopathological analysis found that AOFPs could significantly reduce inflammatory cell infiltration and improve crypt morphology. ELISA and real-time PCR results show that AOFPs can downregulate the contents of TNF-α, IL-1β, and IL-6 and upregulate the content of IL-10. Western blot results show that AOFPs could enhance the expression of E-cadherin, occludin, claudin 1, and ZO-1. In addition, AOFPs improved the richness and diversity of intestinal flora and reshaped the intestinal flora by increasing the proportion of beneficial bacteria and inhibiting the proportion of harmful bacteria. These results indicate that AOFPs have therapeutic effects on UC. This may be due to the regulatory effect of AOFPs on the intestinal flora, restoring intestinal inflammation and permeability.

1. Introduction

Ulcerative colitis (UC) is a chronic nonspecific, noninfectious, inflammatory bowel disease [1]. Its clinical symptoms mainly manifested as hemorrhagic diarrhea, colic abdominal pain, and tenesmus. The UC patients in 2023 were found to be about 5 million cases in the world, and the number will still increase in the future [2]. In practice, the main therapeutic drugs for UC are 5-aminosalicylic acid (5-ASA), prednisone, azathioprine, and infliximab [3]. However, most of them have certain side effects. For example, 5-ASA could induce severe myocarditis [4]. Due to the drug resistance and prolonged treatment period of infliximab, it increases the risk of cancer for patients undergoing long-term treatment [5]. Therefore, new and better ways to treat UC need to be found.

The pathogenesis of UC is closely linked to the intestinal barrier, intestinal flora, and immunity. The intestinal barrier composed of intestinal epithelial cells and tight junctions (TJ) is the first defensive site for the invasion of toxoid and pathogenic bacteria, and if the intestinal epithelial cells and TJ are disrupted, excessive oxidative stress and inflammatory reactions can be induced, leading to the deterioration of UC [6, 7]. Research has found that *Agaricus blazei* Murrill polysaccharides attenuate dextran sulfate sodium (DSS)-induced colitis and protect the colon barrier from damage by decreasing MDA, TNF-α, IL-1β, and IL-6 levels and elevating SOD and IL-10 levels [8]. Another research identified

the elevated level of IL-1β leading to increased intestinal TJ permeability, which is an important factor in promoting intestinal inflammation [9].

Besides, disturbance of intestinal flora may lead to impaired intestinal barrier function and immune dysfunction [10]. The richness and diversity of the intestinal flora are significantly reduced in UC patients compared to healthy people, and the level of *Proteobacteria* often significantly increased [11]. In spontaneous colitis mice induced by IL-10 deficiency, the number of *Proteobacteria* in the intestine significantly increases with the development of colitis, indicating that the abundance of *Proteobacteria* is positively correlated with the severity of inflammation [12, 13]. In particular, *Lactobacillus* may alleviate colitis by protecting the intestinal barrier and may also promote the recovery of dysbiosis of the intestinal flora and reduce the inflammatory response caused by intestinal microbial invasion. *Lactobacillus* were found to significantly increase IL-10 levels, inhibit IL-1β, IL-6, and TNF-α levels, and restore TJ protein levels (including ZO-1, bcl-2, and claudin 1) [14].

Alpinia oxyphylla Miq. is a functional food mainly grown in the tropical region. *A. oxyphylla* has been consumed as a dietary supplement for more than 300 years in Yangjiang, China [15]. In folk markets, the fresh fruit of *A. oxyphylla* was processed into various preserved fruits for consumption, such as Jiuzhi Yizhi, sour and sweet Yizhi, Tangsha Yizhi, candied Yizhi, and canned Tangshui Yizhi [16]. *A.* oxyphylla has great potential value in treating intestinal diseases. It is reported that stem and leaf extracts of *A. oxyphylla* can maintain the integrity of the duck's intestinal barrier and regulate intestinal flora [17]. Protocatechuic acid from *A. oxyphylla* promotes the migration and proliferation of human adipose tissue-derived stromal cells (hADSCs), and hADSCs could regenerate the injured tissues, which helps repair the intestinal barrier [18]. Meanwhile, *A. oxyphylla* may be an excellent alternative to steroids and nonsteroidal anti-inflammatory drugs for the treatment of inflammatory diseases [19]. As the main component of *A. oxyphylla* fruit, polysaccharides have been found to possess multiple pharmacological effects. For instance, *A. oxyphylla* fruit polysaccharides (AOFPs) could improve learning and memory capacity in Alzheimer's disease (AD) mice by lowering NO, IL-1β, TNF-α, and PGE-2 levels in AD mice serum [20]. AOFPs significantly could prevent the infection of porcine epidemic diarrhea virus in IPEC-J2 cells [21]. AOFPs have significant immunomodulatory effects on macrophages polarizing [22]. But still now, the research studies of AOFPs on the treatment of UC have not been reported.

The extraction methods of polysaccharides are closely related to their activity. Different extraction methods have significant differences in physicochemical properties and biological activity for polysaccharides. For example, the alkali-extracted *Opuntia macrorhiza* fruit peel polysaccharides have the best inhibitory activity on α-amylase, while the acid-extracted polysaccharides have better antioxidant and antiglycosylation activity [23]. Therefore, the extraction method is an important factor for activity discovery.

In this study, four extraction methods for AOFPs (distilled water, 0.1M NaCl, 0.1M HCl, and 0.1M NaOH) were designed to explore the potential therapeutic effect and mechanism of AOFPs on DSS-induced UC in mice. This study will provide new ideas for the use of AOFPs and the treatment of UC.

2. Materials and Methods

2.1. Materials and Reagents. *A. oxyphylla* fructus were bought from LinShi ShengTai Pharmaceutical Co. Ltd. (Hainan, China). Dextran standards (2, 5, 9, 13, 36, 64, 123, 300, and 2000 kDa) were obtained from the National Institute for Food and Drug Control (Beijing, China). DSS (MW, 36–50 kDa) was provided by MP Biomedicals (Solon, OH, USA). ELISA kits for TNF-α, IL-1β, IL-6, and IL-10 were acquired from Sangon Biotech Co. Ltd. (Shanghai, China). β-Actin (00096360, rabbit, 1 : 5000), claudin 1 (00108074, rabbit, 1 : 2000), occludin (00114087, rabbit, 1 : 2000), ZO-1 (00106956, rabbit, 1 : 2000), E-cadherin (00113481, Rabbit, 1 : 20000) were purchased from Proteintech Group Inc. (Wuhan, China).

2.2. Polysaccharide Preparation and Characterization

2.2.1. Extracting AOFPs Using Different Solvents. The *A. oxyphylla* fructus was ground into powder and sieved through the sieve with a pore diameter of 0.25 mm. Eight hundred grams of *A. oxyphylla* fructus powder was soaked in 95% ethanol at room temperature for 12 h to remove small molecular impurities. After extraction, the *A. oxyphylla* fructus powder was dried at 50°C and used for subsequent experiments.

The extraction method of AOFPs was referenced to that of blackberry polysaccharides [24]. In brief, 200 g *A. oxyphylla* fructus powders were extracted twice with 4000 ml distilled water, 0.1M NaCl, 0.1M HCl, and 0.1M NaOH at 95°C for 2 h, respectively. The extracts were centrifuged at 8000 g for 10 min, the supernatant was collected, and their pH was adjusted to 7.0 with 0.1M HCl or NaOH. Subsequently, the extracts were concentrated to 1/10 of the original volume. Anhydrous ethanol was added to a final concentration of 80%, it was placed at 4°C for 12 h, and the precipitates were dissolved in 400 ml of distilled water. Subsequently, the proteins were removed using Sevag reagent (1-butanol: chloroform, 1 : 4). The supernatants were placed in dialysis membranes (MW: 7000) and dialyzed with distilled water for 48 h. In the end, the four extracts were freeze-dried to give AOFPs. The four AOFPs were named DW, SC, AC, and Al, respectively. Figure 1 shows the extraction flow of AOFPs.

2.2.2. Chemical Composition Analysis. Glucose was used as the standard to determine the total sugar contents at 490 nm according to the phenol-sulfuric acid method [25]. The content of uronic acid was determined using the m-hydroxydiphenyl method at 526 nm with galacturonic acid as the standard [26]. The Coomassie brilliant blue

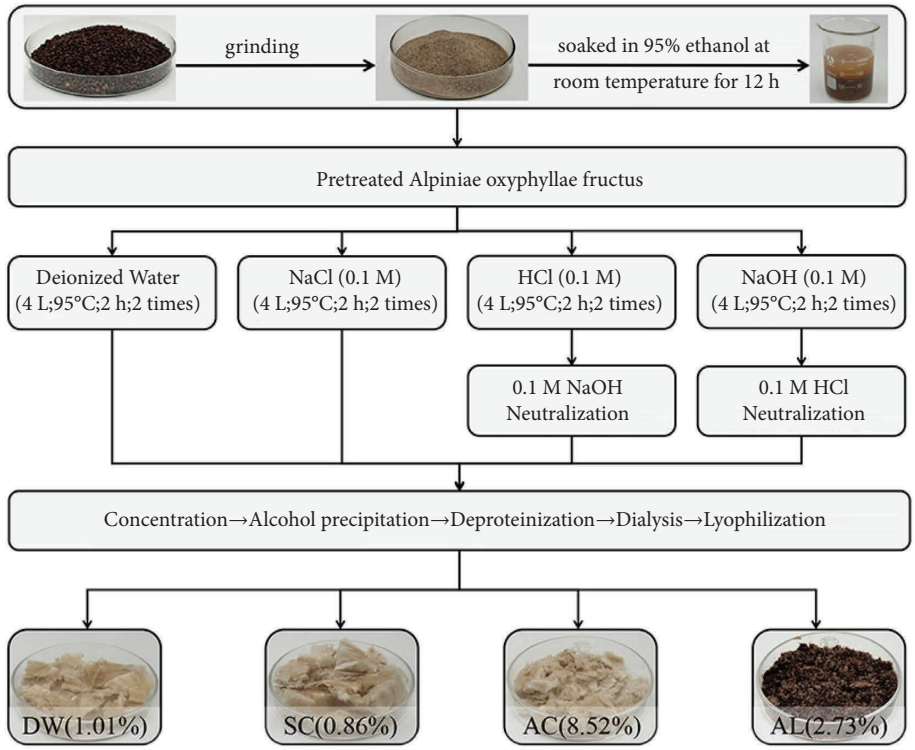

Figure 1: The processes of polysaccharide extracted from *Alpinia oxyphylla* fructus with different extraction solvents.

method was employed to determine the protein content at 595 nm with bovine serum albumin as the standard substance [27].

2.2.3. Monosaccharide Composition Analysis. The monosaccharide composition of AOFPs was analyzed on Waters e2695 liquid chromatography using 1-phenyl-3-methyl-5-pyrazolone (PMP) precolumn derivatization with mannose, rhamnose, glucuronic acid, galacturonic acid, glucose, galactose, xylose, and arabinose as standards [24]. Briefly, 10 mg DW, SC, AC, and Al were added to 2 mL of 4M trifluoroacetic acid (TFA) and hydrolyzed at 105°C for 2 hours, respectively. 1 ml of methanol was added and evaporated at 60°C to remove residual TFA, and then the process was repeated three times. Then, 1 ml of ultrapure water was added to the hydrolysate to dissolve it. Then, 500 μl of hydrolysate was taken and 500 μl of NaOH (0.3 M) and 500 μl of PMP solution (0.5 M) were added sequentially, mixed, and put into a water bath at 70°C for 1 h. After cooling to room temperature, 500 μl HCl (0.3 M) was added and then extracted 3 times with chloroform. The same derivatization steps were performed for mixtures of standard monosaccharides. A C18 column (4.6 × 250 mm) was used to analyze the AOFPs samples and standard solutions. The 84% phosphate buffer solution (0.08 M, pH = 6.8) and 16% acetonitrile were used as mobile phases, and the flow rate was set to 1 ml/min.

2.2.4. Molecular Weight (MW) Determination. The molecular weight distribution of DW, SC, AC, and AL was determined on Shimadzu LC-2010 liquid chromatography. The system was equipped with the RID-20A (SHIMADZU, Japan). TSK gel G4000PWXL (300 × 7.8 mm, 7 μm) column was used as a chromatographic column for molecular weight determination. Ultrapure water was added to the AOFPs to obtain 1 mg/ml polysaccharide solutions. Samples were fed in volumes of 10 μl. Ultrapure water was used as the mobile phase with a flow rate of 0.5 ml/min. Dextran standards were used to produce standard curves and calculate the molecular weight of AOFPs based on the standard curve [28].

2.2.5. Fourier Transform-Infrared (FT-IR) Spectroscopy Analysis. KBr (100 mg) was added to DW, SC, AC, and AL (1 mg), respectively, and then ground and compressed. AOFPs were analyzed in the range of 4000–400 cm^{-1} using FT-IR spectroscopy (IS50, Thermo Fisher, USA).

2.2.6. Ultraviolet Spectrum (UV) Analysis. DW, SC, AC, and AL were prepared as 1 mg/ml polysaccharide solutions and scanned at 200–600 nm using an ultraviolet-visible spectrophotometer.

2.2.7. Triple Helical Structure Analysis. The triple helix structure of AOFPs was determined using the Congo red test [29]. 1 mg/ml of DW, SC, AC, and AL solutions was prepared using ultrapure water. Each polysaccharide solution (2 ml) was added with 80 μm/L Congo red solution (2 ml). After 30 s of stirring, 1 mol/L NaOH was added sequentially to make the NaOH concentration of the mixed solutions 0, 0.1, 0.2, 0.3, 0.4, and 0.5 M, respectively, and kept 10 min of

light avoidance reaction. The maximum absorption wavelengths were obtained using a UV spectrophotometer measured in the 200–800 nm range.

2.2.8. Zeta Potential Analysis. The Zeta potential of AOFP solutions (1 mg/ml) was measured by using a NanoBrook 90Plus PALS (Brookhaven, USA).

2.2.9. Scanning Electron Microscopy (SEM) Analysis. The microcosmic appearance of DW, SC, AC, and AL was observed by an SEM (Sigma 300, Zeiss, Germany) at the accelerated voltage of 10.00 kV.

2.3. Animal Experiments. Male C57BL/6J mice (6 weeks old, 15–18 g) were purchased from Tianqin Biotechnology Co., Ltd. (Changsha, China). The animals were adaptively raised for 7 days in a temperature and light control room with a humidity of 55% ($22 \pm 2^{\circ}$C, 12-hour cycle) and freely obtained distilled water and food. All animal experiments were performed in accordance with the National Research Council's Guide for the Care and Use of Laboratory Animals. All experimental procedures were approved by the Ethics Committee of Hainan Medical University (permit no. HYLL-2022-278).

2.3.1. Modelling and Administration of UC Mice. After 7 days of adaptation, mice were randomly divided into 7 groups ($n = 10$): control group (CON), model group (MOD), positive drug group (POS), DW group (DW), SC group (SC), AC group (AC), and AL group (AL). The CON group drank distilled water, while the other six groups provided distilled water containing 3% DSS. At the same time, the model group was intragastrically administered with distilled water, the positive drug group was orally administered with 5-ASA (150 mg/kg), and the DW group, SC group, AC group, and AL group were given corresponding solution (300 mg/kg) for 7 days (Figure 2(a)). On the eighth day, the mice were sacrificed through cervical dislocation and colons were collected, measured, and weighed and then stored at −80°C.

2.3.2. Disease Activity Index (DAI) Scores. During the experiment, all mice were evaluated daily for weight loss, feces consistency, and hematochezia. Briefly, weight loss was calculated as a percentage of the initial body weight 0 (none), 1 (1–5%), 2 (5–10%), 3 (10–20%), and 4 (>20%). The feces consistency score was as follows: 0 (normal), 1 (soft feces), 2 (wet and soft), 3 (loose feces), and 4 (diarrhea). The blood feces score was assessed according to the following criteria: 0 (no blood), 2 (mild blood in the stool), and 4 (severe blood in the stool). DAI scores were determined using the following formula, with higher scores indicating more severe disease.

$$\mathrm{DAI} = \frac{(\text{weight loss score} + \text{feces score} + \text{blood feces fraction})}{3}. \quad (1)$$

2.3.3. Histopathological Analysis. The colons were taken and fixed with tissue fixative and embedded into paraffin. Hematoxylin and eosin (H&E) were used to stain colon sections, and pathological damage in the colon was examined under a microscope. The histological score was assessed according to the following criteria: 0 (normal colonic mucosa), 1 (loss of one-third of crypts), 2 (loss of two-thirds of crypts), 3 (lamina propria covered with a single layer of epithelial cell, with mild inflammatory cell infiltration), and 4 (erosions and marked inflammatory cell).

2.3.4. Determination of MPO, SOD, and MDA in the Colons of Mice. According to the instructions in the kits, the colon tissue sample was added to the corresponding solution, and then it was homogenized with a homogenizer and centrifuged at 5000 g for 10 min at 4°C and the supernatant was collected for detection.

2.3.5. ELISA Measurement. Prechilled PBS (0.01 M, pH 7.4) was added to the clipped colonic tissue. After homogenization, the sample was centrifuged (5000 g, 10 min) at 4°C. The supernatant was taken for cytokine analysis. The levels of IL-1β, IL-6, TNF-α, and IL-10 were measured using commercial ELISA kits.

2.3.6. Real-Time PCR Analysis. Eastep® Super Total RNA Extraction Kit (Promega, Shanghai, China) was used to extract total RNA from the colon tissue. Hifair® III 1 Strand cDNA Synthesis Super Mix for qPCR (Yeasen, Shanghai, China) was used to reverse transcribe RNA into cDNA. Then, template DNA and primers were added to the Hieff® qPCR SYBR Green Master Mix (Yeasen, Shanghai, China) and quantified using the CFX96 Touch Real-Time PCR Detection System (Bio-Rad, USA). Genes involving TNF-α, IL-1β, IL-6, and IL-10 were determined. To measure the mRNA expression level, β-actin was used as an endogenous control, and the relative expression level was calculated using the $2^{-\Delta\Delta Ct}$ method [30]. The primer sequences of mouse were designed and are listed in Table 1.

2.3.7. Western Blot. RIPA lysate and protease inhibitor were added to the colon tissue, homogenized, and placed at 4°C for 1 h for lysis and then centrifuged at 12,000 g for 15 min, and the supernatant was taken as the protein sample. BCA protein assay kit (Biosharp, Hefei, China) was used to determine protein concentration in samples and subsequently adjusted with RIPA so that the concentrations of each group of samples were consistent. 5 × DSD loading buffer was added to the samples and then boiled in boiling water at 100°C for 5 min to denature the proteins. Groups of proteins were separated by electrophoresis and transferred to 0.45 μm polyvinylidene difluoride (PVDF) membranes (Millipore Corporation, MA, USA). PVDF membranes were blocked with 5% skim milk powder for 2 h, washed with Tris-buffered saline with Tween 20 (TBST), and incubated with primary antibody at 4°C overnight and then washed again with TBST and incubated with secondary antibody for 1 h. Finally,

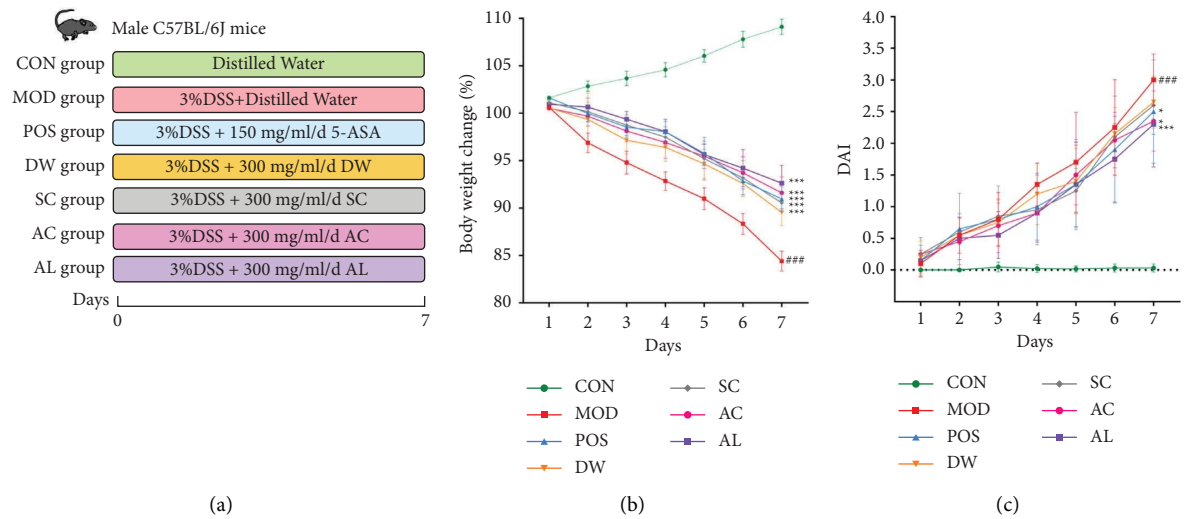

Figure 2: Experimental design and the effect of AOFPs on DSS-induced UC mice. (a) Modelling and treatment plans in animal experiments. (b) Body weight change. (c) DAI scores. Data are represented as mean ± SD ($n = 10$). $^{###}P < 0.001$ compared with the control group. $^{*}P < 0.05$, $^{***}P < 0.001$ compared with the model group.

Table 1: Primer sequences.

Gene		Sequence (mouse)
TNF-α	Forward	5′-CGCTGAGGTCAATCTGC-3′
	Reverse	5′-GGCTGGGTAGAGAATGGA-3′
IL-6	Forward	5′-ACAGAAGGAGTGGCTAAGGA-3′
	Reverse	5′-AGGCATAACGCACTAGGTTT-3′
IL-1β	Forward	5′-AGTTGACGGACCCCAAA-3′
	Reverse	5′-TCTTGTTGATGTGCTGCTG-3′
IL-10	Forward	5′-GCCCTTTGCTATGGTGTC-3′
	Reverse	5′-TCTCCCTGGTTTCTCTTCC-3′
GAPDH	Forward	5′-GATGGACACATTGGGGTT-3′
	Reverse	5′-AAAGCTGTGGCGTGATG-3′

PVDF membranes were washed 3 times with TBST and then developed with a chemiluminescence kit (Beyotime Biotechnology, Shanghai, China). The expression levels of proteins were quantified and normalized to the relative expression levels of β-actin.

2.3.8. Intestinal Flora Analysis. Collected fecal samples were used for intestinal flora analysis. DNA was extracted from the microbiome of mice feces. The 16S rRNA gene in bacteria was amplified by using TransStart® FastPfu DNA Polymerase (Transgen, Beijing, China). PCR products were recovered and purified with the AxyPrep DNA gel extraction kit (Axygen, USA). The MiSeq library was built by using TruSeq™ DNA Sample Prep Kit (San Diego, CA, USA). Then, MiSeq was sequenced on Illumina MiSeq PE300 platform of Shanghai Majorbio Biopharm Technology Co., Ltd. (Shanghai, China).

Intestinal microbiota analysis was conducted by UPARSE (version 7.0.1090), all sequences were divided into OTUs based on different similarity levels, and bioinformatics analysis was performed on OTUs at 97% similarity levels. Based on the results of the OTU clustering analysis, the α-diversity analysis was calculated by Mothur (version 1.30.2). The results of α-diversity analysis were tested for intergroup differences using one-way ANOVA. β-Diversity analysis was performed by principal coordinates analysis (PCoA) and β-diversity was calculated by the Bray–Curtis distance. LDA effect size (LEfSe) analysis was performed using the nonparametric Kruskal–Wallis (KW) sum-rank test to detect the species richness differences between different groups and obtain significantly different species, and then the Wilcoxon rank-sum test was used to test the consistency of differences between different species in subgroups of different groups in the previous step, and finally LDA (linear discriminant analysis) was used to estimate the impact of these different species on the differences between groups. The relationship between the microbes with inflammation and intestinal barrier was analyzed using Spearman's rank correlation test. With the 16S rRNA gene amplicon sequencing results, PICRUST2 (version 2.2.0) was used for KEGG pathway analysis of the intestinal flora.

2.4. Data Analysis. Statistical significance among groups was analyzed using Student's t-test or one-way ANOVA in GraphPad Prism version 9.4.1 (GraphPad Software, Inc., San Diego, CA, USA). All data were expressed as the mean ± standard error of the mean (SEM). Differences of P values <0.05 were considered statistically significant.

3. Results

3.1. Extraction Yields and Physicochemical Properties of AOFPs. In this research, four water-soluble polysaccharides were extracted from the *A. oxyphylla* fructus by different extraction solvents. Extraction rates and physicochemical properties vary depending on the extraction solution. It can be seen from Table 2 that the yield of AOFPs varies according to the extraction solvent (about 0.86%–8.52%).

Table 2: Extraction yields, chemical properties, and compositions of AOFPs from *A. oxyphylla* by using four extraction solvents.

Item	Sample			
	DW	SC	AC	AL
Yield (%)	1.01	0.86	8.52	2.73
Total sugar (%)	21.56	28.97	71.82	64.74
Uronic acid (%)	74.17	63.15	3.42	8.72
Protein (%)	0.25	0.12	0.31	2.32
Monosaccharide composition (molar ratio, %)				
Mannose	0.84	0.76	0.10	1.06
Rhamnose	2.78	2.96	0.47	2.87
Glucuronic acid	2.74	2.75	0.14	2.30
Galacturonic acid	32.37	23.23	1.22	3.51
Glucose	26.24	35.91	97.07	40.00
Galactose	8.81	8.67	0.42	9.42
Xylose	12.63	12.39	0.46	16.39
Arabinose	13.59	13.33	0.12	24.45

Among them, acid solution (AC, 8.52%) is the highest, which may be due to the fact that the glycosidic bonds in this AOF are more easily hydrolyzed by acid [31]. The yield of alkali solution (AL, 2.73%) was the second highest, and this may be due to the fact that alkaline solutions easily disrupt or hydrolyze cell walls, causing polysaccharides to diffuse [32]. The study's results corroborate with those of Ulva intestinalis sulfated polysaccharides [33]. The extraction rate of water solution (DW, 1.01%) was not significantly different from that of salt solution (SC, 0.86%).

The highest total sugar content was found in AC (71.82%). It is possible that the glycosidic bonds were destroyed in the acidic environment at high temperatures [24]. The contents of uronic acid were more in DW (74.17%) and SC (63.15%) and less in AC (3.42%) and Al (8.72%), which means they are all acidic polysaccharides. The protein content of DW, SC, and AC is relatively low (0.12–0.31%). Perhaps this is the result of solvent extraction reducing the isolated proteins in these AOFPs. However, the highest protein content was found in AL (2.32%). This may be due to the fact that hydrogen bonds were easily broken in alkaline environments, promoting protein production [34].

3.2. Structure Characterizations of AOFPs

3.2.1. Monosaccharide Composition. By comparing the retention time with the standard sample, the monosaccharides in the AOFPs were determined. As shown in Figure 3(a) and Table 2, AOFPs contain mannose, rhamnose, glucuronic acid, galacturonic acid, glucose, galactose, xylose, and arabinose. The experimental results showed that all four AOFPs contained these eight monosaccharides, but there were differences in their molar ratios. Different solution environments have different degrees of hydrogen bond disruption and partial degradation of polysaccharide molecules, resulting in different percentages of each monosaccharide in the four AOFPs. The contents of glucuronic acid and galacturonic acid in AC and AL were lower, while the content of glucose was higher. This may be due to the degradation of uronic acid into small molecule sugars in an acidic or alkaline environment. Comparing the content of uronic acid measured data, the results were consistent [35].

3.2.2. Molecular Weight Determination. It was obvious from Figure 3(b) that the MWs of the AOFPs were different based on the extraction method. Similar peaks were found in DW and SC, both with a single symmetry, and their MWs were 921.87 kDa and 748.35 kDa, respectively. In AC, two populations around molecular weights of 1675.7 kDa (3.21%) and 4.22 kDa (96.79%) were found. The latter one indicates the presence of oligosaccharides, meaning that the polysaccharides were degraded. AL presented two main peaks with the MWs of 1099.86 kDa (97.08%) and 621.90 kDa (2.92%).

3.2.3. FT-IR Analysis. Analysis of the distinctive functional groups of polysaccharides through FT-IR is frequent. The FT-IR spectra of AOFPs revealed the typical features of polysaccharides, as illustrated in Figure 3(c). The broadly stretched intense peaks at 3405 cm^{-1} represented the stretching of the –OH, and the absorption areas at 2950 cm^{-1} were caused by C-H stretching and bending vibrations [36]. The absorbance areas of 1744 cm^{-1} represented the symmetric stretching vibration of the C=O in acetyl groups, and it was observed only in DW and SC. The absorbance areas of 1613 cm^{-1} represented the COO- deprotonated carboxyl group, implying that galacturonic acid was detected in the samples [24]. The absorption region at 1415 cm^{-1} was due to the stretching vibration of the C-O [37]. The absorption areas at 1099 cm^{-1} and 1010 cm^{-1} were due to the stretching vibration of the pyranose ring [36]. Moreover, the peaks at 862 cm^{-1} represented the presence of a β-glycoside bond [38].

3.2.4. UV Analysis. Ultraviolet-visible analysis can be used to determine the purity of extracted polysaccharides [39]. In Figure 3(d), there are no obvious absorption peaks for DW, SC, AC, and AL at 260 nm and 280 nm, indicating that there are fewer nucleic acid substances or free proteins. These findings agree with those of the chemical composition study.

3.2.5. Triple Helical Structure Analysis. The Congo red experiment is able to judge whether the AOFPs contain triple helix structures. If the sample has the triple helix structure, the λ_{max} will be red-shifted [29]. According to Figure 3(e), as the concentration of NaOH gradually magnified, the λ_{max} values of DW, SC, and AC were red-shifted, which suggested DW, SC, and AC had a triple helical conformation. On the contrary, the trend of the λ_{max} of Al was similar to that of the control, so it was judged that AL did not have a triple helix structure.

3.2.6. Zeta Potential Analysis. Zeta potential is a key indicator of the strength of the attractive and repulsive forces of macromolecules in solution and reflects the stability of polysaccharide solutions. As the absolute value of zeta

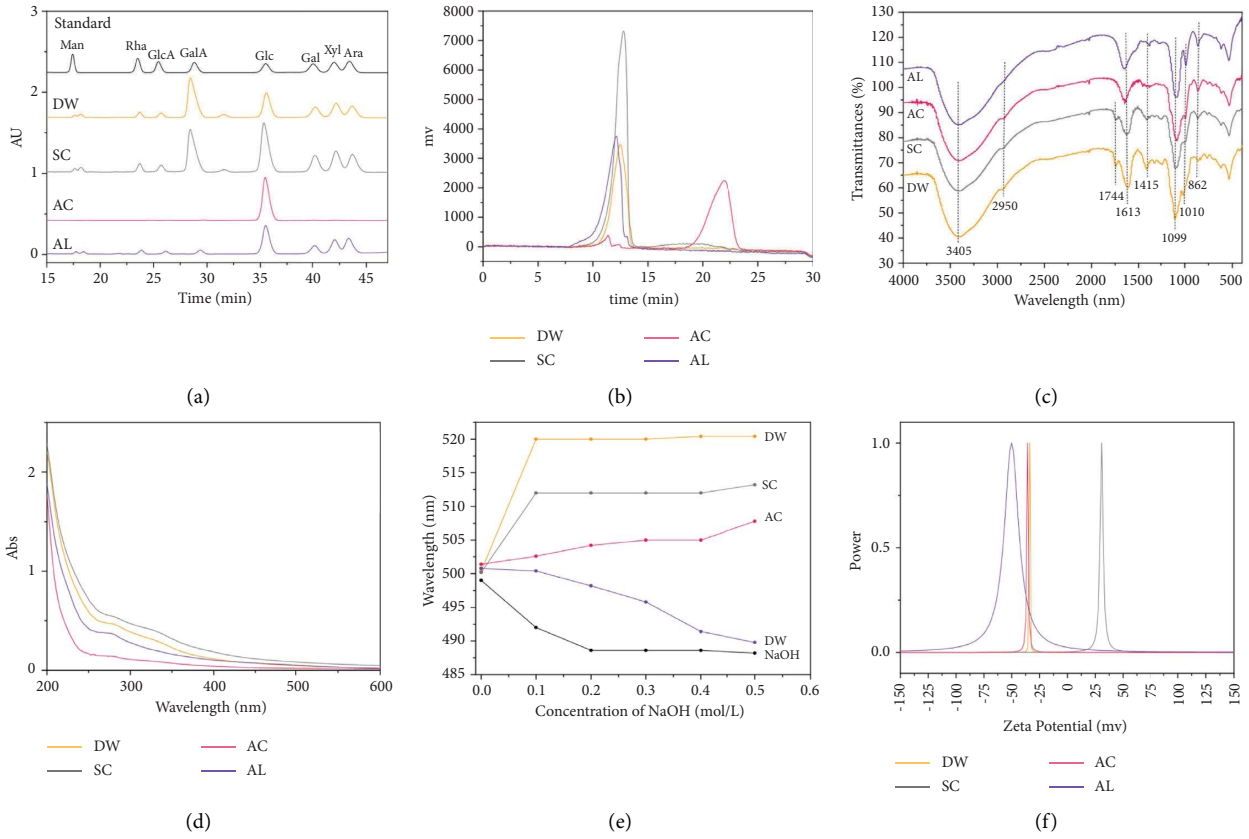

Figure 3: The physicochemical properties of AOFPs. (a) HPLC chromatograms of PMP derivatives of standard monosaccharides and AOFPs. (b) Molecular weight distribution curve. (c) FT-IR spectra. (d) UV spectra. (e) λ_{max} of Congo red and Congo red-AOFPs complex. (f) Zeta spectra.

potential increases, the stability of the polysaccharide solution gradually becomes stronger. Therefore, the zeta potentials of the four polysaccharides were determined [40, 41]. The results in Figure 3(f) show that the Zeta potentials of DW, SC, AC, and AL are −33.82 mV, 30.65 mV, −35.78 mV, and −50.14 mV, indicating that they have good stability. DW, AC, and AL were negatively charged, implying that they are all anionic polysaccharides. However, SC was positively charged, indicating that the structure of polysaccharide may be modified in NaCl solvent.

3.2.7. SEM Analysis. SEM can be used to observe the surface morphology of polysaccharides. As shown in Figure 4, the four polysaccharides are all in lamellar structure, in which the DW surface is distributed with dense irregular caves. SC surface is rough, with different sizes of depressions. The surface of AC and AL is smooth. This may be due to the different solutions used to extract polysaccharides, resulting in differences in the indicated structures of AOFPs [42].

3.3. Effect of AOFPs on DSS-Induced UC Mice

3.3.1. Effects of AOFPs on Body Weight and DAI Scores in UC Mice. In order to study whether AOFPs have potential therapeutic effects on UC, this study fully evaluated the clinical symptoms of the mouse UC model induced by DSS, such as weight loss, diarrhea, and bloody stool. Figure 2(b) shows that, during the experiment, the weight of the CON group mice continued to increase, while the weight of the MOD group significantly decreased. All five treatment groups alleviated this trend. Figure 2(c) shows that POS, DW, SC, SC, and AL groups alleviated these phenomena and significantly improved the DAI score. The results indicate that DSS-induced mice exhibited significant UC characteristics, such as weight loss, increased DAI score, decreased colon length, and histological changes. This is consistent with the report, indicating that the UC mouse model was fruitfully established [43]. After treatment with AOFPs, these symptoms have been alleviated to varying degrees, with the most significant efficacy seen with AL. The results indicate that AOFPs have therapeutic effects on UC and there are differences in their efficacy.

3.3.2. Effects of AOFPs on Colonic Length and Histopathology in UC Mice. Colonic mucosal ulceration, inflammatory cell infiltration, crypt structure change, and colon shortening were frequently seen in the colon of UC mice [44]. As seen in Figure 5(a), the colonic length of mice fed with 3% DSS solution was significantly shortened. POS, DW, SC, SC, and AL groups can alleviate this phenomenon, in which the AL group has the best effect. According to the H&E staining

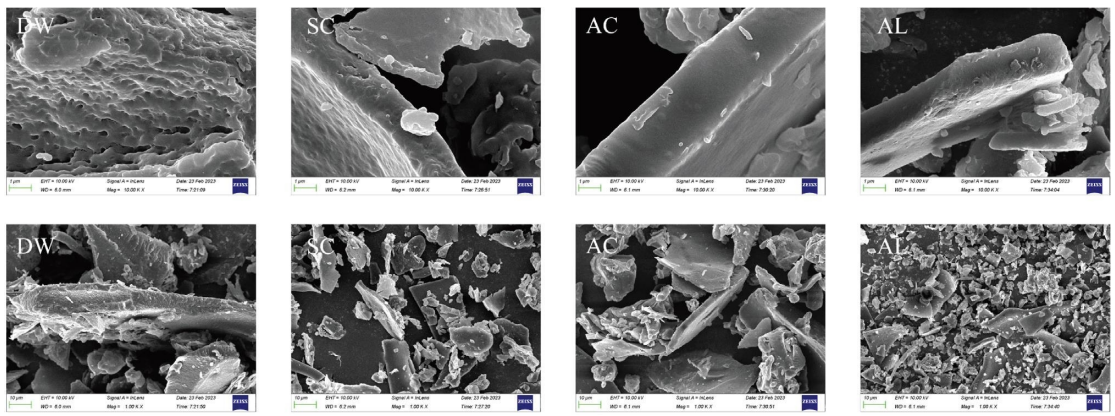

Figure 4: SEM photographs of AOFPs.

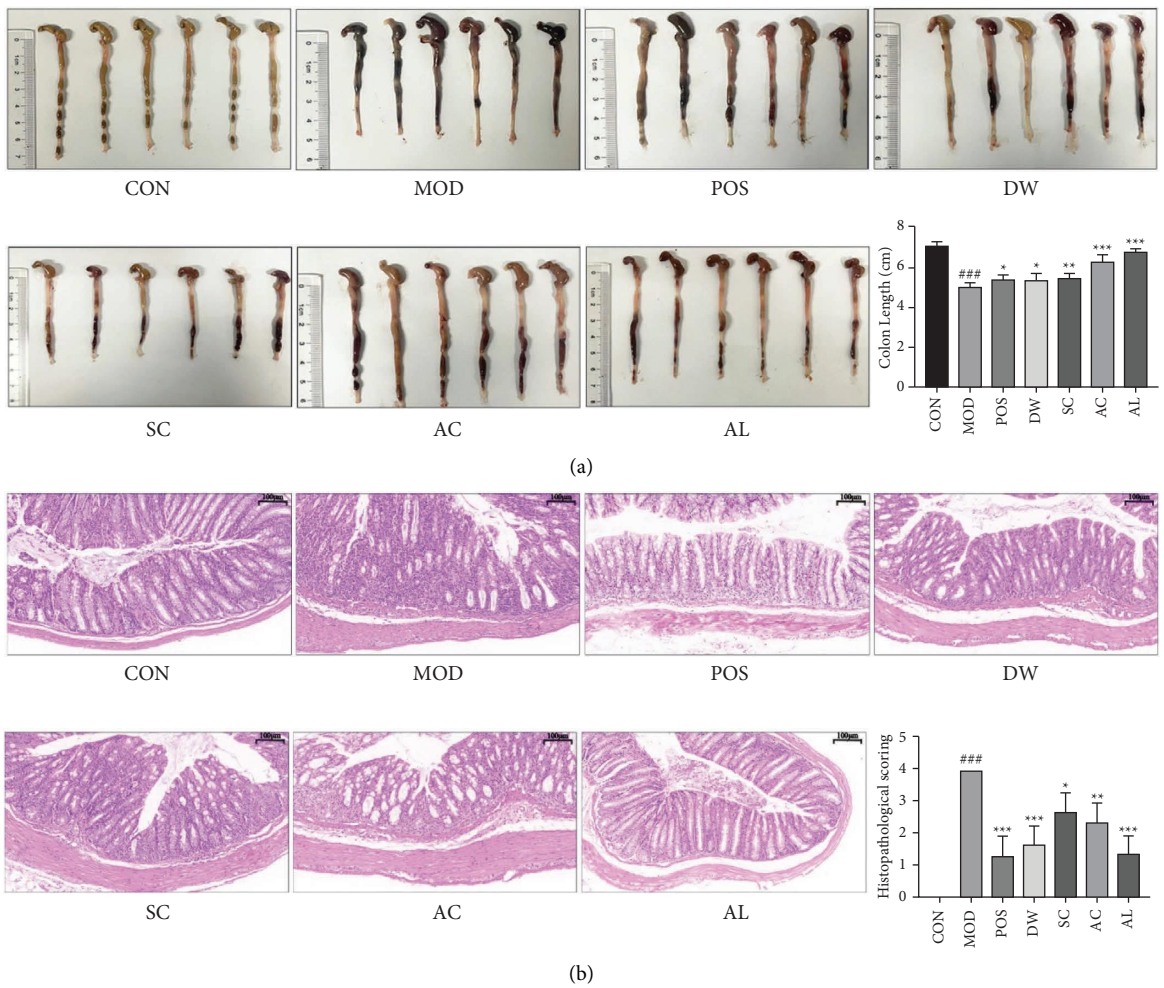

Figure 5: Effects of AOFPs on colon length and histomorphology in DSS-induced colitis mice. (a) Colon length and images of each group. (b) Histopathological score and representative H&E staining images. Data are represented as mean ± SD ($n = 6$). $^{###}P < 0.001$ compared with the control group. $^{*}P < 0.05$, $^{**}P < 0.01$, and $^{***}P < 0.001$ compared with the model group.

results of the colon in Figure 5(b), the muscularis, mucosa, and crypt structures of the colon in the CON group were normal, and a large number of goblet cells were visible. In the MOD group, the crypt structure was distorted, goblet cells were significantly reduced, mucosa edema and other tissue damage were observed, and there was obvious inflammation in colon tissue. In addition, the POS, DW, SC, SC, and AL groups can reduce the pathological damage of

these tissues to varying degrees, in which the AL group has the best effect. These results suggest that AOFPs can effectively protect the colon from DSS-induced length shortening and inflammation.

3.3.3. Effect of AOFPs on the Level of Oxidative Stress in the Colon of UC Mice. To identify changes in colonic oxidative stress levels before and after treatment with AOFPs, SOD activity, MPO levels, and MDA levels were measured experimentally. As shown in Figure 6(a), DSS intervention resulted in a decrease in colon SOD levels, while POS, AC, and AL were able to significantly restore SOD levels ($P < 0.05$). As shown in Figure 6(b), DSS intervention induced an increase in MPO levels in the colon, but after POS, SC, AC, and AL treatment, MPO levels significantly decreased ($P < 0.05$). As shown in Figure 6(c), compared with the CON group, the level of MDA in the MOD group increased, but DW, SC, AC, and AL alleviated this change in varying degrees ($P < 0.05$). According to the experimental results, after treatment with AOFPs, the levels of SOD, MPO, and MDA have been restored, indicating that AOFPs can remove oxygen free radicals, repair oxidative damage to the mucosal barrier, and alleviate inflammatory symptoms, with AL having the best antioxidative stress effect.

3.3.4. Effect of AOFPs on the Expression of Inflammatory Factors. Abnormal upregulation of proinflammatory cytokines is one of the hallmarks of UC [45]. To obtain information about the changes in inflammatory factor levels in the intestine of mice before and after treatment with AOFPs, we measured the expression of IL-1β, IL-6, IL-10, and TNF-α in colonic tissues by ELISA kits and real-time PCR. As depicted in Figure 7, the gene expression of IL-1β, IL-6, and TNF-α was significantly higher in the MOD group than in the CON group ($P < 0.05$). Nevertheless, this tendency was prominently reversed after treatment with POS, DW, SC, AC, and AL ($P < 0.05$). When compared to the CON group, IL-10 gene expression was dramatically reduced in the MOD group, while it prominently elevated following treatment with POS, DW, SC, AC, and AL ($P < 0.05$).

3.3.5. Effects of AOFPs on DSS-Induced Colon Barrier Integrity in UC Mice. To determine whether AOFPs have an ameliorative effect on the intestinal barrier in UC mice, levels of E-cadherin and TJ protein (including claudin 1, occludin, and ZO-1) were measured in colonic tissue by Western blot. The protein level in the MOD group was much lower than it was in the CON group, showing that the intestinal barrier had been compromised. As shown in Figure 8, DSS induces significant downregulation of claudin 1, occludin, ZO-1, and E-cadherin. DW significantly upregulated all four proteins. SC significantly upregulated occludin, ZO-1, and E-cadherin. AC significantly upregulated claudin 1 and ZO-1. AL only significantly upregulated ZO-1.

3.3.6. Effect of AOFPs on Intestinal Flora of UC Mice

(1) Changes in the Diversity of the Intestinal Flora. To explore the changes in intestinal flora of UC mice before and after AOFP treatment, 16S rRNA gene sequencing analysis was used to compare the intestinal flora of seven groups. With the increase of sequencing number, it was observed that the sparse curve of the Shannon index gradually tends to be stable, and the coverage index exceeded 0.9979 (Figure 9(a)), demonstrating that the sequencing data were adequate and trustworthy for further study. The overall number of OTUs and the number of distinct OTUs in each group can be represented visually using the Venn diagram [46], so that we used the Venn diagram (Figure 9(b)) to analyze the number of OTUs in the sample. There are 228 in each group, while the DW, SC, AC, and AL groups had 2, 1, 0, and 3 OTUs different from the other groups, respectively.

The richness and diversity of intestinal flora were determined by α-diversity analysis [47]. ACE and Chao reflect the species richness of communities in a single sample. ACE is used to estimate the index of the number of OTUs in the community. The Chao value rises as the overall number of species increases. The Simpson index embodies the diversity of microorganisms. The higher the Simpson index value, the better the community diversity. Sobs is the number of OTUs observed. It can be seen from Figure 9(c) that the ACE and Chao indexes of the MOD group are noticeably lower than those of the CON group. The ACE and Chao indexes of the POS and DW groups were significantly greater than those of the MOD group, showing that DW can mitigate the decline in species richness brought on by DSS. The Simpson index of the AL group was remarkably higher than that of the MOD group, indicating that AL can increase community diversity. The Sobs index of the MOD group was lower than that of the CON group. The Sobs index of the POS and DW groups dramatically rose in comparison with the MOD group. In β-analysis, PCoA is frequently used to identify differences within and between groups of samples. In Figure 9(d), there was a clear distance between the MOD and CON groups, indicating that DSS can significantly alter the intestinal flora of mice. Meanwhile, there was a certain distance between the treatment groups and the MOD group, demonstrating that 5-ASA and AOFP treatment had altered the bacterial community structure in UC mice.

(2) Changes in Intestinal Flora Composition. According to Figure 10(a), the intestine microbiota of mice consisted mainly of *Firmicutes*, *Verrucomicrobiota*, *Bacteroidota*, *Proteobacteria*, and *Actinobacteria*. Of these, *Firmicutes* and *Bacteroidota* are dominant phyla in healthy individuals [48]. According to Figures 10(b) and 10(c), in the CON group, the value of F/B was 2.26, and after DSS treatment, F/B increased to 5.64, while POS (F/B = 4.11), DW (F/B = 1.39), SC (F/B = 1.23), AC (F/B = 1.68), and AL (F/B = 3.50) significantly suppressed this trend ($P < 0.05$). DSS led to a decrease in the relative abundance of *Bacteroidota*, while DW, SC, and AC significantly reversed this trend. In Figures 10(d) and 10(e), DSS led to an enhancement in the relative abundance of *Proteobacteria* and *Actinobacteria* when compared to the

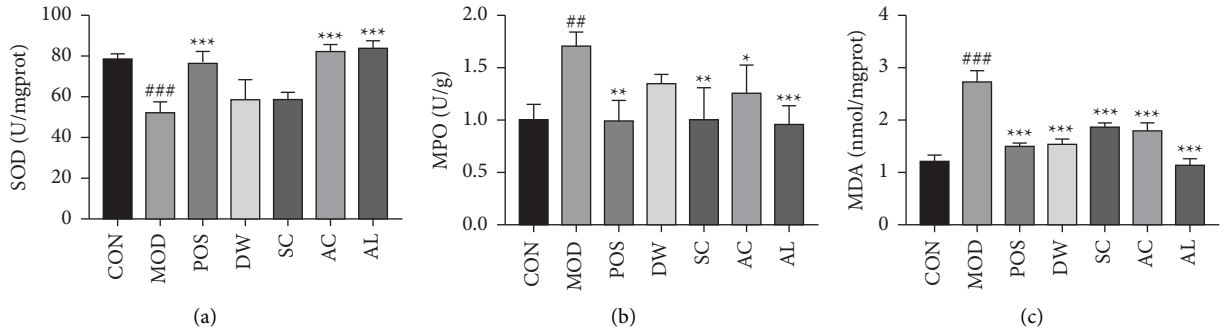

Figure 6: Effect of AOFPs on oxidative stress markers in DSS-induced colitis mice. The levels of (a) SOD, (b) MPO, and (c) MDA. Data are presented as the means ± SD ($n = 6$). $^{\#\#}P < 0.01$ and $^{\#\#\#}P < 0.001$ compared with the control group. $^{*}P < 0.05$, $^{**}P < 0.01$, and $^{***}P < 0.001$ compared with the model group.

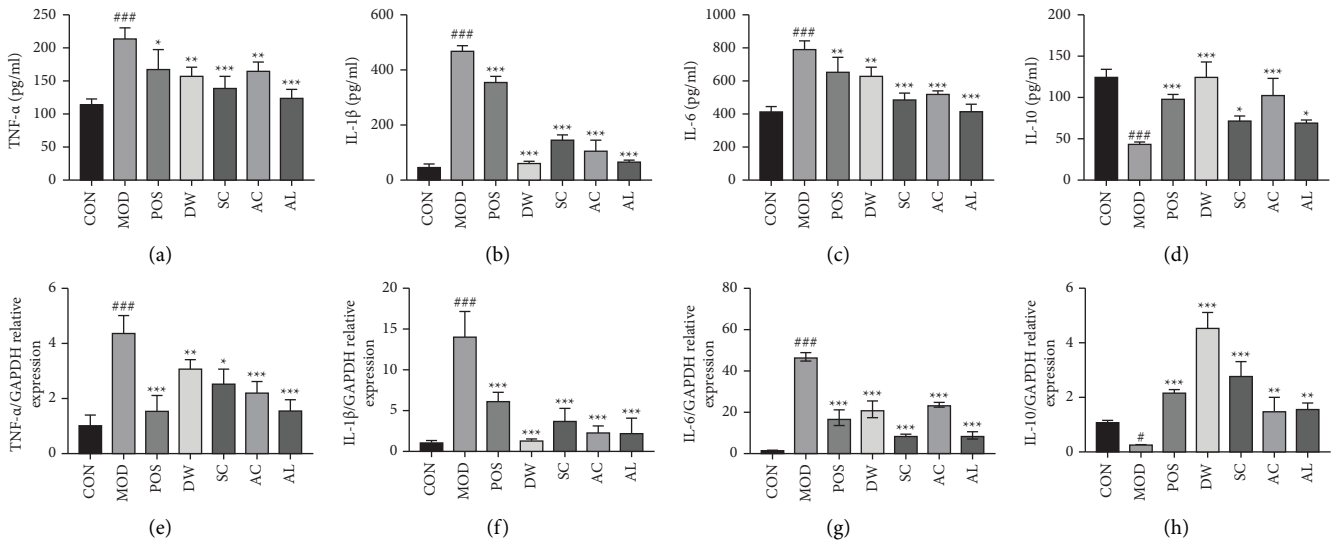

Figure 7: Effect of AOFPs on inflammatory cytokines in DSS-induced colitis mice. The levels of (a) TNF-α, (b) IL-1β, (c) IL-6, and (d) IL-10 in mice colons. Relative mRNA expression of (e) TNF-α, (f) IL-1β, (g) IL-6, and (h) IL-10. Data are presented as the means ± SD ($n = 6$). $^{\#}P < 0.05$, $^{\#\#}P < 0.01$, and $^{\#\#\#}P < 0.001$ compared with the control group. $^{*}P < 0.05$, $^{**}P < 0.01$, and $^{***}P < 0.001$ compared with the model group.

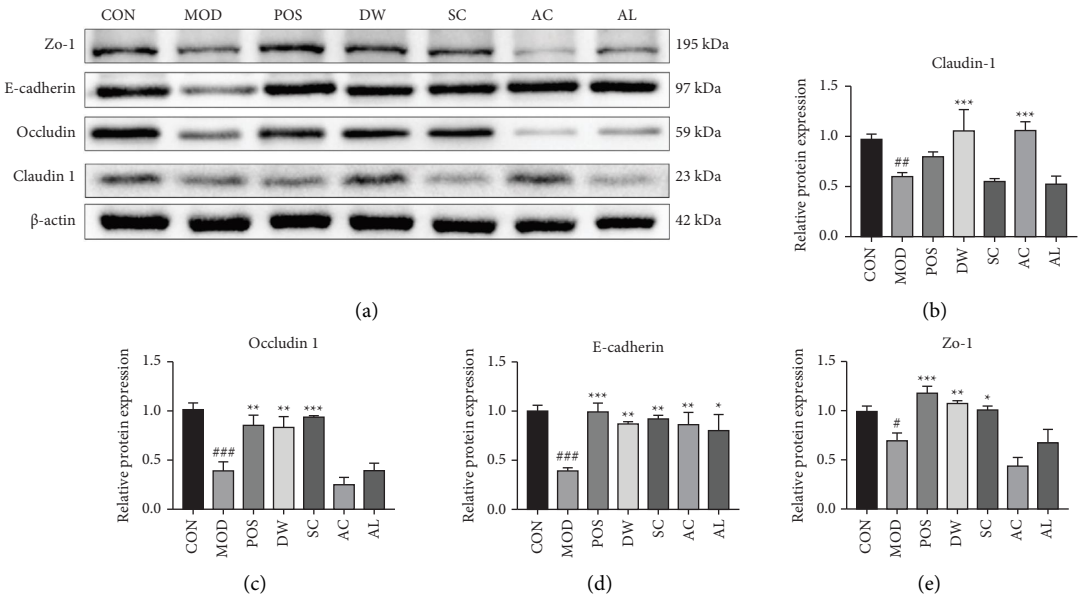

Figure 8: Effect of AOFPs on TJ protein and E-cadherin in DSS-induced colitis mice. (a) Immunoblot analysis of claudin 1, occludin, E-cadherin, and ZO-1 protein extracts from colon tissue samples. The levels of (b) claudin 1, (c) occludin, (d) E-cadherin, and (e) ZO-1 in mice colons. Data are presented as the means ± SD ($n = 3$). $^{\#}P < 0.05$, $^{\#\#}P < 0.01$, and $^{\#\#\#}P < 0.001$ compared with the control group. $^{*}P < 0.05$, $^{**}P < 0.01$, and $^{***}P < 0.001$ compared with the model group.

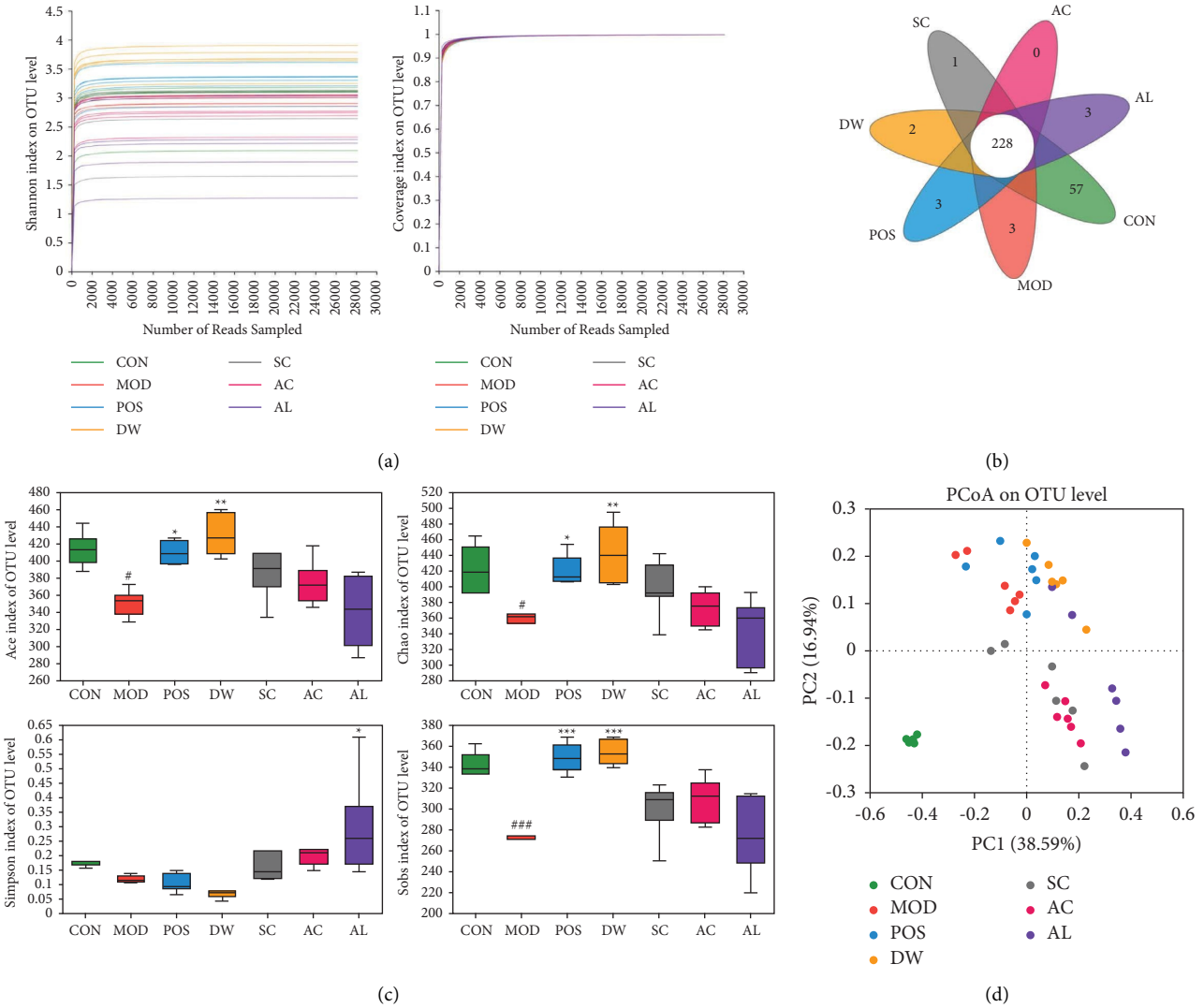

Figure 9: AOFPs altered microbial diversity. (a) Rarefaction curves includes Shannon index and Coverage index. (b) A Venn diagram between seven groups. (c) The alpha diversity includes Ace index, Chao index, Simpson index, and Sobs index. (d) PCoA. Data are presented as the mean ± SD ($n = 6$). $^{\#}P < 0.05$ and $^{\#\#\#}P < 0.001$ compared with the control group. $^{*}P < 0.05$, $^{**}P < 0.01$, and $^{***}P < 0.001$ compared with the model group.

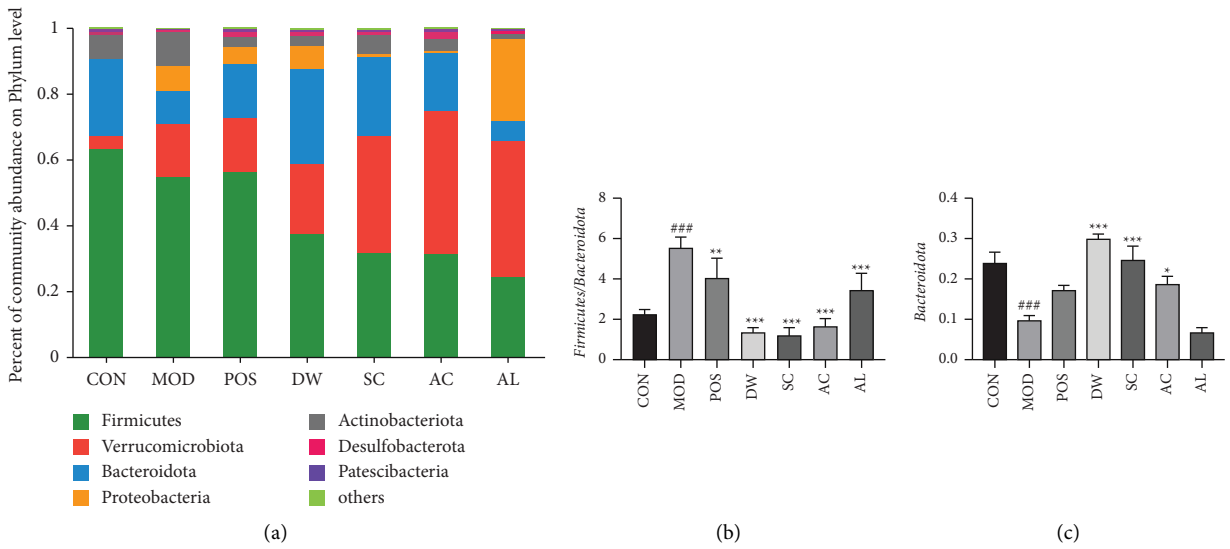

Figure 10: Continued.

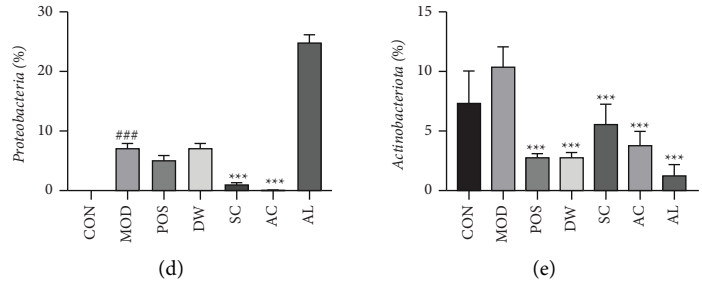

Figure 10: AOFPs alters microbial composition on the phylum level. (a) Compositions of the microbial community on the phylum level. (b) The ratio of *Firmicutes* to *Bacteroidota*. (c) The relative abundance of *Bacteroidota*. (d) The relative abundance of *Proteobacteria*. (e) The relative abundance of *Actinobacteria*. Data are presented as the mean ± SD ($n = 6$). $^{###}P < 0.001$compared with the control group. $^{*}P < 0.05$ and $^{***}P < 0.001$ compared with the model group.

CON group. However, DW, SC, AC, and AL significantly reduced the relative abundance of *Actinobacteria*. SC and AC significantly reduced the relative abundance of *Proteobacteria*.

The heat map analysis (Figure 11(a)) was carried out at the genus level. Figures 11(b)–11(g) display a few example species, and in the MOD group, the relative abundance of harmful bacteria significantly increased. After treatment with 5-ASA and AOFPs, the relative abundance of *norank_f__Muribaculaceae* and *norank_f__Lachnospiraceae* increased significantly, the relative abundance of *Escherichia-Shigella*, *Bifidobacterium*, *Romboutsia*, *Turicibacter*, and *Faecalibaculum* in the MOD group significantly reduced.

In order to further identify the differences between dominant and characteristic bacteria in each group, the linear discriminant analysis (LDA) of the effect amount (LEfSe) was performed. LEfSe is used to detect features with significant differences in abundance and identify groups with significant differences in abundance. The LDA discrimination column chart counts the microbial groups with significant effects in multiple groups. The LDA score was obtained through LDA analysis (linear regression analysis). The higher the LDA score, the greater the species richness's impact on the difference effect. Figures 12(a) and 12(b) show the microbial communities with significant effects in each group, with LDA values greater than 3. The results showed that, at the genus level, the species richness of *Bifidobacterium*, *Romboutsia*, *Turicibacter*, and *Faecalibaculum* in the MOD group had a greater impact on the difference effect. The species with the highest LAD values in the POS, DW, SC, AC, and AL groups are *norank_f__norank_o__Clostridia_UCG-014, Rikenellaceae_RC9_gut_group*, *Akkermansia*, and *Escherichia-Shigella*, respectively.

(3) Correlation Analysis of Intestinal Flora with Inflammation and Intestinal Barrier. In order to better understand the relationship between the abundance of intestinal flora and colitis indicators in mice, a correlation analysis was conducted between microbe, inflammatory factors, and intestinal barrier. As shown in Figure 13(a), *Romboutsia*, *Turicibacter*, *Faecalibaculum*, and *Coriobacteriaceae_UGG-002* were positively and significantly correlated with TNF-α, IL-6, and IL-1β. *Lachnoclostridium*, *norank_f__Muribaculaceae*, and *Eubacterium_fissicatena_group* were negatively correlated with IL-1β and positively correlated with IL-10. In addition, *Bacteroides*, *Alistipes*, and *Odoribacter* were positively correlated with IL-6. As shown in Figure 13(b), *norank_f__Muribaculaceae* showed a positive correlation with E-cadherin and claudin 1 expression. *Escherichia-Shigella* showed a negative correlation with claudin 1 expression. *Bacteroidetes* showed a positive correlation with ZO-1 expression. *Turicibacter* showed a negative correlation with E-cadherin expression. These results suggest that inflammation and intestinal barrier were closely related to the imbalance of intestinal flora in UC mice.

(4) Prediction of Changes in the Function of the Intestinal Flora. The KEGG pathway of intestinal flora was analyzed by PICRUST 2 (version 2.2.0) based on the sequencing results of 16S rRNA gene amplifiers. As shown in Figure 14, we found significant abnormalities in the metabolic microbiota of intestinal DSS, such as a decrease in carbohydrate metabolism, amino acid metabolism, energy metabolism, and an increase in membrane transport and signal transport. However, DW, SC, and AC treatment can significantly correct these abnormal changes and improve the dysfunction of intestinal flora in UC mice. However, no significant difference in pathway was found in the AL group.

4. Discussion

The etiology of UC is complex, and multiple studies have suggested that it may be related to epithelial barrier dysfunction, inflammation, and intestinal flora [11, 49]. *A. oxyphylla* is beneficial for intestinal health and can repair the intestinal barrier and regulate intestinal bacteria [17]. In this research, we used deionized water, NaCl, HCl, and NaOH solutions to obtain *A. oxyphylla* polysaccharides and investigated the therapeutic effects of AOFPs on DSS-induced UC mice. The results showed that there are significant differences in the monosaccharide composition, molecular weight, FT-IR spectra, surface morphology, triple helix structure, and Zeta potential of polysaccharides obtained by different extraction methods. The polysaccharides obtained from different extraction solvents were evaluated at

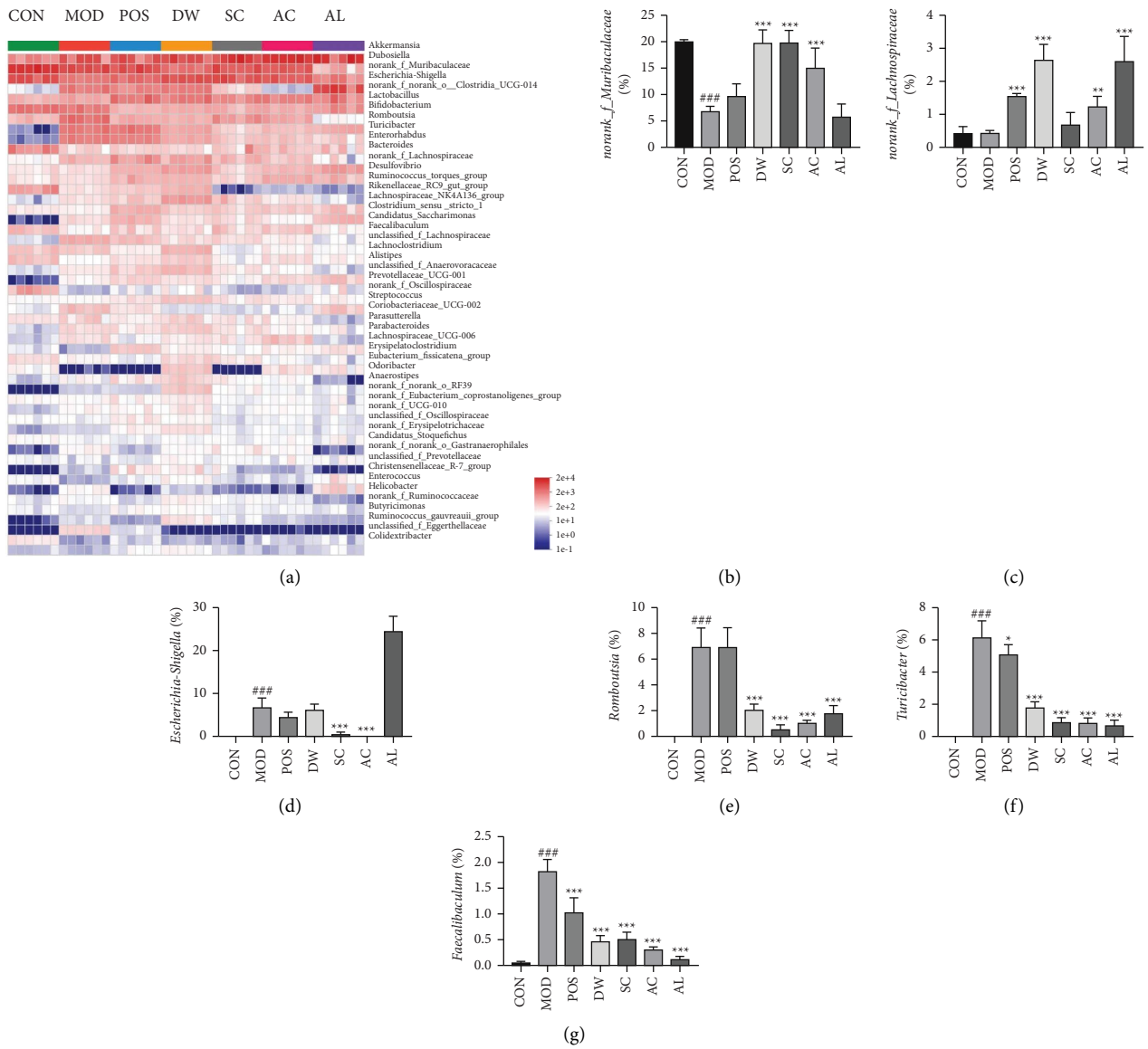

FIGURE 11: AOFPs alters microbial composition on the genus level. (a) Community heatmap on the genus level. The relative abundance of (b) *norank_f__Muribaculaceae*, (c) *norank_f__Lachnospiraceae*, (d) *Escherichia-Shigella*, (e) *Romboutsia*, (f) *Turicibacter*, and (g) *Faecalibaculum*. Data are presented as the mean ± SD ($n = 6$). $^{###}P < 0.001$ compared with the control group. $^{**}P < 0.01$ and $^{***}P < 0.001$ compared with the model group.

the same dose, to explore the differences in the therapeutic effects of AOFPs on UC.

DSS can impair the integrity of the colon barrier and downregulate the expression of TJ protein, improve the permeability of the intestinal mucosa to endotoxin and antigens, and induce a fierce inflammatory response [45, 50]. TJ proteins in the intestinal epithelium, including claudin 1, occludin, and ZO-1, are important factors for the inflammation relief and mucosal repair process in ulcerative colitis [51]. E-cadherin is a cell adhesion protein that plays a crucial role in maintaining the shape of intestinal epithelial cells, villus morphology, and barrier function. The loss of E-cadherin could lead to the destruction of intestinal tissue structure, which is related to the damage of the location and function of goblet cells and Paneth cells, the reduction of the expression of antibacterial factors, and the insufficient clearance of intestinal pathogens [52]. In addition, in DSS-induced UC mice and E-cadherin-deficient mice exhibited more severe weight loss, dehydration, and bloody stool symptoms, which were significantly associated with more severe acute inflammation [52]. In this experiment, it can be seen that DSS can significantly reduce the levels of claudin 1, occludin, ZO-1, and E-cadherin in colon tissue, while the AOFPs restore their expression to varying degrees, indicating that AOFPs have a protective effect on the intestinal barrier.

The balance between anti-inflammatory (IL-10) and proinflammatory (IL-1β, IL-6, and TNF-α) cytokines is an important factor in maintaining intestinal health. TNF-α can promote the increase of IL-6 and IL-1β, while large amounts

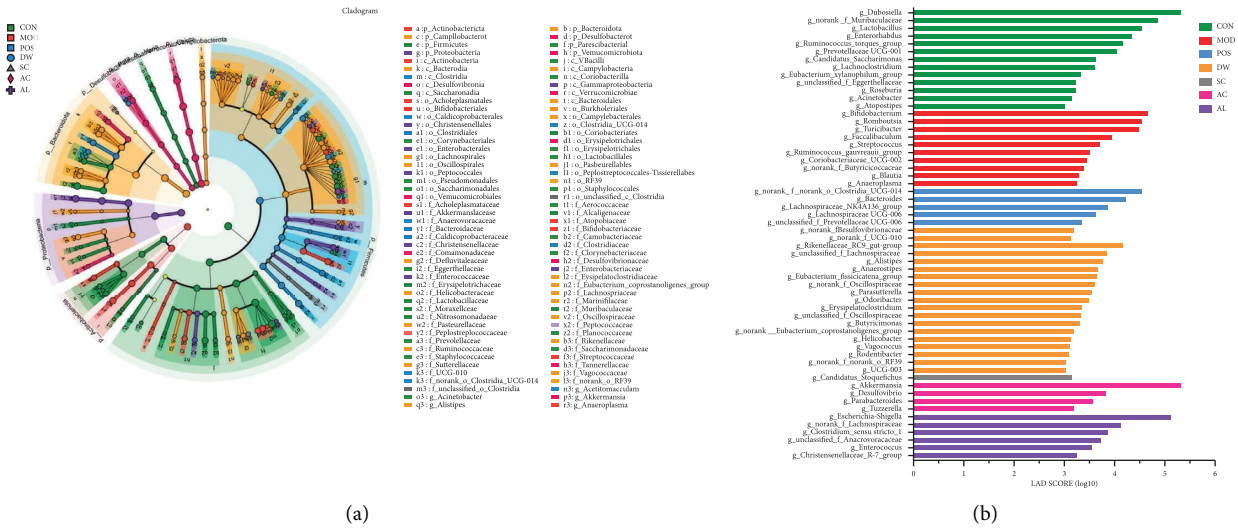

FIGURE 12: LEfSe analysis. (a) LEfSe cladogram (the rings, from outer to inner, represent genus, family, order, class, and phylum). (b) LEfSe histogram (LDA scores >3) at the genus level.

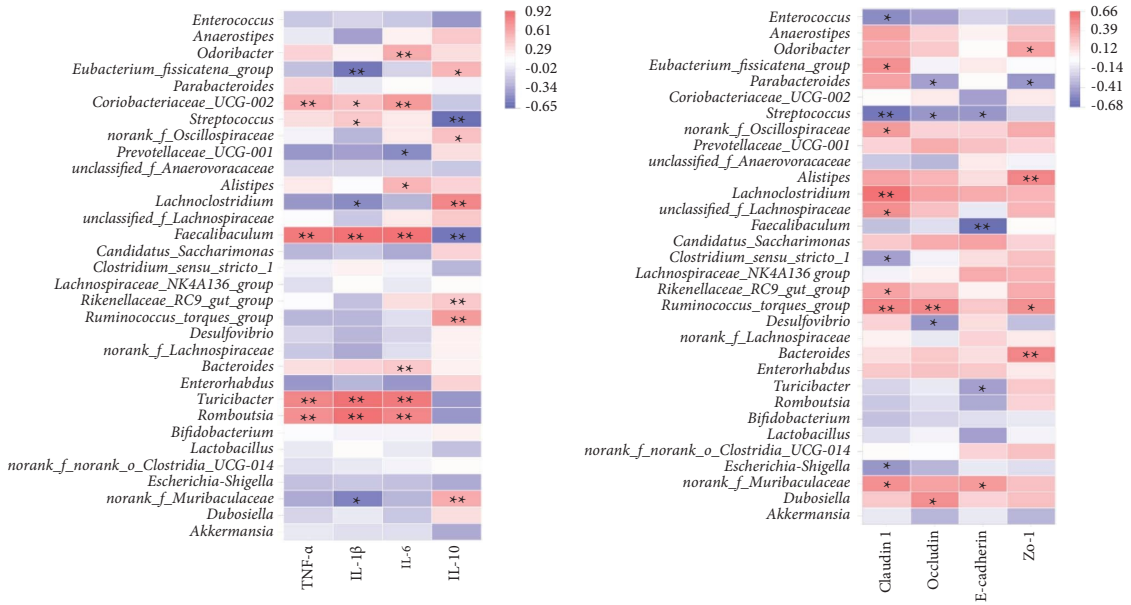

FIGURE 13: Heatmap correlation analysis of: (a) intestinal flora and inflammatory factors and (b) intestinal flora and intestinal barrier. Data are presented as the mean ± SD ($n = 6$). $^{*}P < 0.05$ and $^{**}P < 0.01$.

of TNF-α, IL-6, and IL-1β may lead to increased intestinal inflammation, thereby disrupting the intestinal mucosal barrier [53, 54]. IL-10 can inhibit the production of proinflammatory cytokines. Loss of IL-10 receptor expression can disrupt the regulatory role of macrophages and promote the spontaneous development of severe colitis [55]. In our study, AOFPs reduced the level of TNF-α, IL-6, and IL-1β and increased the level of IL-10, which indicated that inflammation in the colon has been alleviated after AOFP treatment.

When UC occurs, it is often accompanied by oxidative stress reactions, and previous studies have shown that excessive oxygen free radicals could promote the development of colitis and barrier damage [54, 56]. SOD is a metal ion-rich protein with powerful antioxidant effects, which converts superoxide anion radicals into oxygen and hydrogen peroxide. Therefore, SOD plays a crucial role in antioxidant activity and is also an important indicator for evaluating antioxidant activity [46]. MPO is a peroxidase with pro-oxidant and proinflammatory effects. Its activity in the colon is closely related to neutrophil infiltration. Therefore, its level can reflect the degree of mucosal damage [54, 57]. MDA reflects the intensity of lipid peroxidation in the body and indirectly shows the extent of tissue

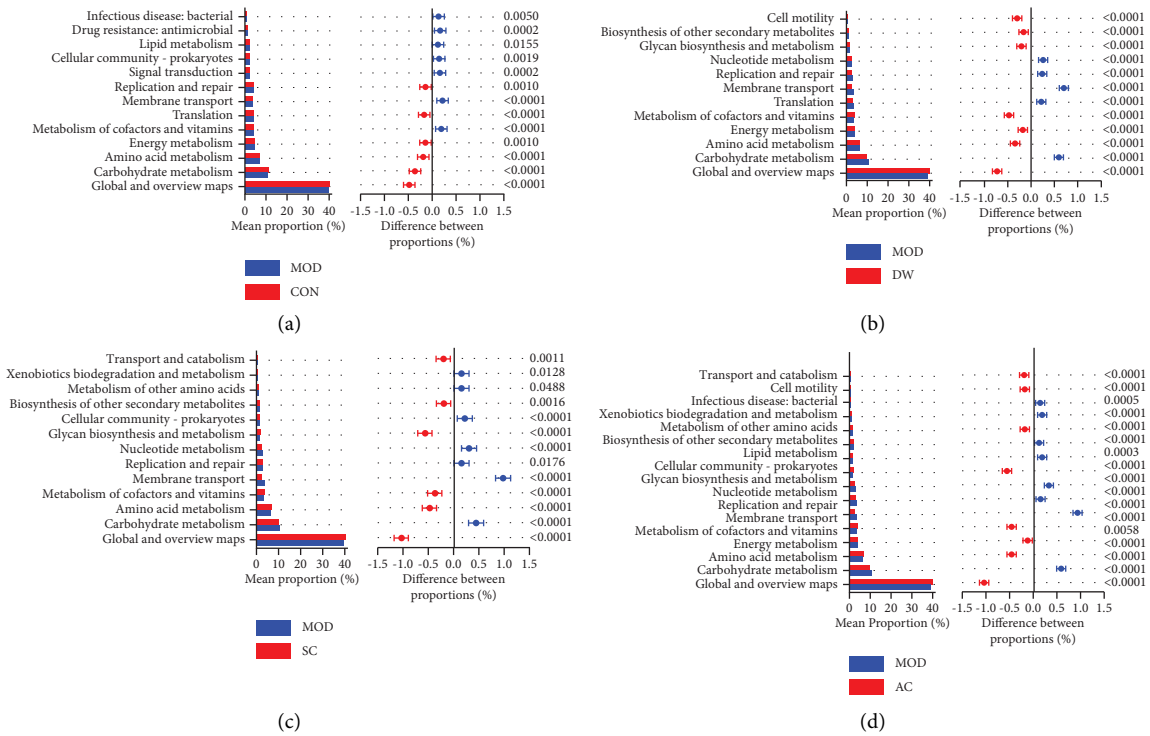

Figure 14: Analysis of differences in KEGG metabolic pathways between groups. (a) MOD vs CON. (b) MOD vs DW. (c) MOD vs SC. (d) MOD vs AC.

peroxidative damage [58]. Through this research, we found AOFPs could increase the level of SOD and decreased the levels of MPO and MDA. These results indicated that AOFPs have a good protective effect on DSS-induced colonic oxidative damage.

Intestinal flora is closely related to the development of UC. Previous research has confirmed that DSS could lead to a decrease in the diversity and richness of intestinal flora in mice [59]. At the phylum level, the ratio of *Firmicutes* to *Bacteroidota* (F/B) is a crucial marker for assessing these alterations. Disturbance of intestinal flora can lead to an increase in F/B values [60]. The research report proved that Octadecanol-H treatment can reduce the F/B ratio of mice, which may be related to the anti-inflammatory effect of *Bacteroidota* [61, 62]. In our study, AOFPs also presented a reduced F/B ratio and increased the relative abundance of *Bacteroidota*. This indicated that the regulatory effect of polysaccharides at the phylum level may be one of the reasons for their anti-inflammatory effects. *Proteobacteria* is a biomarker for microbial imbalance and the risk of UC [63]. The intestinal inflammation deteriorated with the increase of the relative abundance of *Proteobacteria* [12]. SC and AC could significantly reduce the relative abundance of *Proteobacteria*, which is beneficial for the stability of intestinal flora.

Research has found that the balance of intestinal flora levels is closely related to intestinal permeability, such as increasing the relative abundance of *Bacteroides, Faecalibaculum,* and *Turicibacter* and reducing the relative abundance of *Desulfovibrio, Lactobacillus, Lachnospiraceae*, *Alistipes*, and Enterorhabdus, which will lead to an increase in intestinal mucosal permeability [47]. The *Bifidobacterium bifidum* significantly enhances the intestinal TJ barrier in mice in a Toll-like receptor-2-dependent manner and protects the permeability of the mouse colon from DSS damage [64]. Another study found that the relative abundance of *norank_f__Muribaculaceae* was downregulated, while the relative abundance of *Streptococcus*, *Escherichia-Shigella*, *Romboutsia*, *Turicibacter*, and *Faecalibaculum* is upregulated, which is related to the alteration of intestinal inflammation [65]. After treatment with AOFPs, we also found that intestinal flora was reversed at the genus level, such as an increase in the relative abundance of *norank_f__Muribaculaceae* and *norank_f__Lachnospiraceae* and a decrease in the relative abundance of *Escherichia-Shigella*, *Romboutsia*, *Turicibacter*, and *Faecalibaculum*, indicating that AOFPs can restore the imbalance of gut microbiota caused by DSS.

In order to discover the contribution of intestinal flora to colitis, we conducted a correlation analysis between differential microbiota and inflammation and permeability indicators. Through correlation analysis, we found *Romboutsia*, *Turicibacter*, *Faecalibaculum*, and *Coriobacteriaceae_UCG-002* were significantly positively correlated with TNF-α, IL-6, and IL-1β. The results indicated an increase in the proportion of these microbiota promotes the deterioration of intestinal inflammation. The correlation analysis results between microbiota and intestinal permeability indicators show that beneficial bacteria such as *norank_f_Muribaculaceae* were positively correlated with claudin 1 and E-cadherin, while *Streptococcus* was significantly negatively correlated with claudin 1, occludin, and E-

cadherin. These results suggested that polysaccharides may improve intestinal permeability by upregulating the *norank_f_Muribaculaceae* and downregulating *Streptococcus*. Due to the inconsistent regulation of the intestinal flora by the four types of AOFPs, their anti-inflammatory effects and barrier repair capabilities vary. For example, there is a significant correlation between *Turicibacter, Faecalibaculum*, and anti-inflammatory factors. In the AL group, the relative abundance of *Turicibacter* and *Faecalibaculum* is closest to that of the CON group, and AL exhibits the best anti-inflammatory effect in ELISA and real-time PCR results. However, the regulatory effect of AL on other bacterial communities is not ideal, and its ability to repair the intestinal barrier is not as good as other AOFPs. There is a significant correlation between *norank_f__Muribaculaceae*, *norank_f__Lachnospiraceae*, and claudin 1. DW has the strongest upregulation ability towards them. In western blot results, DW had the strongest recovery effect on claudin 1.

In addition, the overall function of the intestinal flora also varies with the composition of the intestinal flora proportion. Previous research found that intestinal flora in the DSS group can enhance the signal transduction and membrane transport capacity of bacteria and reduce the biosynthesis of other secondary metabolites and glycan biosynthesis and metabolism pathways [66]. Our research results found that oral administration with DW, SC, and AC could significantly increase the biosynthesis of other secondary metabolites and reduce membrane transport. This indicates that AOFPs may contribute to the recovery of intestinal flora function.

Through the gut microbiota analysis of AOFPs, we found that they play a comprehensive role in regulating gut inflammation and barrier function by regulating the levels of gut microbiota. Among them, AL has a strong regulatory effect on the bacterial community of intestinal inflammation, while DW has a strong regulatory effect on intestinal permeability.

5. Conclusions

In this study, we obtained four different polysaccharides through deionized water, NaCl, HCl, and NaOH extraction. At the same time, their physicochemical properties and structural characteristics were analyzed. Animal experiments have verified the therapeutic effect of AOFPs on colitis induced by DSS. According to the results, we speculate that AOFPs have treated UC by regulating the intestinal flora to repair the intestinal barrier and inhibit intestinal inflammation.

Data Availability

The data used to support the findings of this study are available from the corresponding author upon request.

Ethical Approval

The animal study protocol was approved by the Ethics Committee of Hainan Medical University (permit no. HYLL-2022-278).

Disclosure

The funding body had no role in the design of the study, collection, analysis, and interpretation of data, and writing the manuscript.

Conflicts of Interest

The authors declare no conflicts of interest.

Authors' Contributions

X.M. and Y.L. conceptualized the study; Y.W. was responsible for methodology; Y.T. was responsible for software; L.L. and D.D. validated the data; G.M. performed formal analysis; Q.Z. investigated the data; Y.T. and Y.L. were responsible for resources and involved in funding acquisition; X.H. performed data curation and study supervision; X.M. visualized the study and prepared the original draft; Y.L. reviewed and edited the manuscript and was involved in project administration. All authors have read and agreed to the published version of the manuscript.

Acknowledgments

This research was funded by the National Natural Science Foundation of China (nos. 82160826 and 82160795) and Innovative Research Project for Graduate Students at Hainan Medical University (no. HYYS2021A30).

Supplementary Materials

The original image of the western blot is provided in the supplementary material. (*Supplementary Materials*)

References

[1] Z. M. Song, F. Liu, Y. M. Chen, Y. J. Liu, X. D. Wang, and S. Y. Du, "Ctgf-mediated erk signaling pathway influences the inflammatory factors and intestinal flora in ulcerative colitis," *Biomedicine & Pharmacotherapy*, vol. 111, pp. 1429–1437, 2019.

[2] C. Le Berre, S. Honap, and L. Peyrin-Biroulet, "Ulcerative colitis," *The Lancet*, vol. 402, no. 10401, pp. 571–584, 2023.

[3] L. Y. Yao, B. L. Shao, F. Tian et al., "Trends in medication use and treatment patterns in Chinese patients with inflammatory bowel disease," *World Journal of Gastroenterology*, vol. 28, no. 30, pp. 4102–4119, 2022.

[4] K. Fleming, A. Ashcroft, C. Alexakis, D. Tzias, C. Groves, and A. Poullis, "Proposed case of mesalazine-induced cardiomyopathy in severe ulcerative colitis," *World Journal of Gastroenterology*, vol. 21, no. 11, pp. 3376–3379, 2015.

[5] P. Giannos, K. K. Triantafyllidis, G. Giannos, and K. S. Kechagias, "Spp1 in infliximab resistant ulcerative colitis and associated colorectal cancer: an analysis of differentially expressed genes," *European Journal of Gastroenterology and Hepatology*, vol. 34, no. 6, pp. 598–606, 2022.

[6] P. Wu, Y. Su, L. Feng et al., "Optimal dl-methionyl-dl-methionine supplementation improved intestinal physical barrier function by changing antioxidant capacity, apoptosis and tight junction proteins in the intestine of juvenile grass

carp (Ctenopharyngodon idella)," *Antioxidants*, vol. 11, no. 9, p. 1652, 2022.

[7] B. Zheng, M. Ying, J. Xie et al., "A ganoderma atrum polysaccharide alleviated dss-induced ulcerative colitis by protecting the apoptosis/autophagy-regulated physical barrier and the dc-related immune barrier," *Food & Function*, vol. 11, no. 12, pp. 10690–10699, 2020.

[8] Y. Zhang, F. Lu, H. Zhang et al., "Polysaccharides from Agaricus blazei murrill ameliorate dextran sulfate sodium-induced colitis via attenuating intestinal barrier dysfunction," *Journal of Functional Foods*, vol. 92, Article ID 105072, 2022.

[9] L. W. Kaminsky, R. Al-Sadi, and T. Y. Ma, "IL-1β and the intestinal epithelial tight junction barrier," *Frontiers in Immunology*, vol. 12, Article ID 767456, 2021.

[10] M. Ho Do, Y. S. Seo, and H. Y. Park, "Polysaccharides: bowel health and gut microbiota," *Critical Reviews in Food Science and Nutrition*, vol. 61, no. 7, pp. 1212–1224, 2021.

[11] S. Zhu, M. Han, S. Liu, L. Fan, H. Shi, and P. Li, "Composition and diverse differences of intestinal microbiota in ulcerative colitis patients," *Frontiers in Cellular and Infection Microbiology*, vol. 12, Article ID 953962, 2022.

[12] N. R. Shin, T. W. Whon, and J. W. Bae, "Proteobacteria: microbial signature of dysbiosis in gut microbiota," *Trends in Biotechnology*, vol. 33, no. 9, pp. 496–503, 2015.

[13] N. Maharshak, C. D. Packey, M. Ellermann et al., "Altered enteric microbiota ecology in interleukin 10-deficient mice during development and progression of intestinal inflammation," *Gut Microbes*, vol. 4, no. 4, pp. 316–324, 2013.

[14] G. Wang, Q. Xu, X. Jin et al., "Effects of lactobacilli with different regulatory behaviours on tight junctions in mice with dextran sodium sulphate-induced colitis," *Journal of Functional Foods*, vol. 47, pp. 107–115, 2018.

[15] Y. Xie, M. Xiao, Y. Ni et al., "Alpinia oxyphylla Miq. Extract prevents diabetes in mice by modulating gut microbiota," *Journal of Diabetes Research*, vol. 2018, Article ID 4230590, 10 pages, 2018.

[16] Q. Niu, "Study on comprehensive utilization of different parts of medical and edible Alpinia oxyphylla Miq," Master's Thesis, Hainan University, Haikou, China, 2019.

[17] F. Ji, L. Gu, G. Rong et al., "Using extract from the stems and leaves of Yizhi (alpiniae oxyphyllae) as feed additive increases meat quality and intestinal health in ducks," *Frontiers in Veterinary Science*, vol. 8, Article ID 793698, 2021.

[18] H. Wang, T. Q. Liu, S. Guan, Y. X. Zhu, and Z. F. Cui, "Protocatechuic acid from Alpinia oxyphylla promotes migration of human adipose tissue-derived stromal cells in vitro," *European Journal of Pharmacology*, vol. 599, no. 1-3, pp. 24–31, 2008.

[19] S. H. Yu, H. J. Kim, S. Y. Jeon et al., "Anti-inflammatory and anti-nociceptive activities of Alpinia oxyphylla miquel extracts in animal models," *Journal of Ethnopharmacology*, vol. 260, Article ID 112985, 2020.

[20] W. Shi, J. Zhong, Q. Zhang, and C. Yan, "Structural characterization and antineuroinflammatory activity of a novel heteropolysaccharide obtained from the fruits of Alpinia oxyphylla," *Carbohydrate Polymers*, vol. 229, Article ID 115405, 2020.

[21] Y. Chen, Y. Zhang, Q. Luo et al., "Inhibition of porcine epidemic diarrhea virus by alpiniae oxyphyllae fructus polysaccharide 3," *Research in Veterinary Science*, vol. 141, pp. 146–155, 2021.

[22] X. Yang, S. Zhou, H. Li et al., "Structural characterization of alpiniae oxyphyllae fructus polysaccharide 2 and its activation effects on Raw264.7 macrophages," *International Immunopharmacology*, vol. 97, Article ID 107708, 2021.

[23] S. Amamou, H. Lazreg, J. Hafsa et al., "Effect of extraction condition on the antioxidant, antiglycation and A-amylase inhibitory activities of Opuntia macrorhiza fruit peels polysaccharides," *LWT-Food Science and Technology*, vol. 127, Article ID 109411, 2020.

[24] Z. M. Dou, C. Chen, Q. Huang, and X. Fu, "Comparative study on the effect of extraction solvent on the physicochemical properties and bioactivity of blackberry fruit polysaccharides," *International Journal of Biological Macromolecules*, vol. 183, pp. 1548–1559, 2021.

[25] M. Dubois, K. A. Gilles, J. K. Hamilton, P. A. Rebers, and F. Smith, "Colorimetric method for determination of sugars and related substances," *Analytical Chemistry*, vol. 28, no. 3, pp. 350–356, 1956.

[26] N. Blumenkrantz and G. Asboe-Hansen, "New method for quantitative determination of uronic acids," *Analytical Biochemistry*, vol. 54, no. 2, pp. 484–489, 1973.

[27] C. He, R. Zhang, X. Jia et al., "Variation in characterization and probiotic activities of polysaccharides from litchi pulp fermented for different times," *Frontiers in Nutrition*, vol. 9, Article ID 993828, 2022.

[28] H. Chen, J. Zeng, B. Wang et al., "Structural characterization and antioxidant activities of bletilla striata polysaccharide extracted by different methods," *Carbohydrate Polymers*, vol. 266, Article ID 118149, 2021.

[29] X. Guo, J. Kang, Z. Xu et al., "Triple-helix polysaccharides: formation mechanisms and analytical methods," *Carbohydrate Polymers*, vol. 262, Article ID 117962, 2021.

[30] T. Li, R. R. Chen, H. P. Gong et al., "FGL2 regulates IKK/NF-κB signaling in intestinal epithelial cells and lamina propria dendritic cells to attenuate dextran sulfate sodium-induced colitis," *Molecular Immunology*, vol. 117, pp. 84–93, 2020.

[31] C. Fang, G. Chen, and J. Kan, "Comparison on characterization and biological activities of mentha haplocalyx polysaccharides at different solvent extractions," *International Journal of Biological Macromolecules*, vol. 154, pp. 916–928, 2020.

[32] Y. Jia, X. Gao, Z. Xue et al., "Characterization, antioxidant activities, and inhibition on alpha-glucosidase activity of corn silk polysaccharides obtained by different extraction methods," *International Journal of Biological Macromolecules*, vol. 163, pp. 1640–1648, 2020.

[33] N. Peasura, N. Laohakunjit, O. Kerdchoechuen, and S. Wanlapa, "Characteristics and antioxidant of Ulva intestinalis sulphated polysaccharides extracted with different solvents," *International Journal of Biological Macromolecules*, vol. 81, pp. 912–919, 2015.

[34] J. K. Yan, Z. C. Ding, X. Gao et al., "Comparative study of physicochemical properties and bioactivity of hericium Erinaceus polysaccharides at different solvent extractions," *Carbohydrate Polymers*, vol. 193, pp. 373–382, 2018.

[35] N. Zhang, B. Yang, K. Mao et al., "Comparison of structural characteristics and bioactivity of tricholoma mongolicum imai polysaccharides from five extraction methods," *Frontiers in Nutrition*, vol. 9, Article ID 962584, 2022.

[36] M. Zhu, R. Huang, P. Wen et al., "Structural characterization and immunological activity of pectin polysaccharide from kiwano (cucumis metuliferus) peels," *Carbohydrate Polymers*, vol. 254, Article ID 117371, 2021.

[37] J. Huo, M. Lei, Y. Zhou et al., "Structural characterization of two novel polysaccharides from gastrodia elata and their

effects on Akkermansia muciniphila," *International Journal of Biological Macromolecules*, vol. 186, pp. 501–509, 2021.

[38] L. Wang, L. Li, J. Gao et al., "Characterization, antioxidant and immunomodulatory effects of selenized polysaccharides from dandelion roots," *Carbohydrate Polymers*, vol. 260, Article ID 117796, 2021.

[39] M. Sfar, G. Souid, F. M. Alminderej et al., "Structural characterization of polysaccharides from coriandrum sativum seeds: hepatoprotective effect against cadmium toxicity in vivo," *Antioxidants*, vol. 12, no. 2, p. 455, 2023.

[40] J. Gu, H. Zhang, H. Yao, J. Zhou, Y. Duan, and H. Ma, "Comparison of characterization, antioxidant and immunological activities of three polysaccharides from sagittaria sagittifolia L," *Carbohydrate Polymers*, vol. 235, Article ID 115939, 2020.

[41] Y. Guo, L. Wang, L. Li et al., "Characterization of polysaccharide fractions from allii macrostemonis bulbus and assessment of their antioxidant," *LWT--Food Science and Technology*, vol. 165, Article ID 113687, 2022.

[42] H. Huojiaaihemaiti, P. Mutaillifu, A. Omer et al., "Isolation, structural characterization, and biological activity of the two acidic polysaccharides from the fruits of the elaeagnus angustifolia linnaeus," *Molecules*, vol. 27, no. 19, p. 6415, 2022.

[43] Y. Ren, Q. Sun, R. Gao et al., "Low weight polysaccharide of hericium Erinaceus ameliorates colitis via inhibiting the Nlrp3 inflammasome activation in association with gut microbiota modulation," *Nutrients*, vol. 15, no. 3, p. 739, 2023.

[44] W. Niu, Y. Dong, Z. Fu et al., "Effects of molecular weight of chitosan on anti-inflammatory activity and modulation of intestinal microflora in an ulcerative colitis model," *International Journal of Biological Macromolecules*, vol. 193, pp. 1927–1936, 2021.

[45] S. Zong, Z. Ye, X. Zhang, H. Chen, and M. Ye, "Protective effect of lachnum polysaccharide on dextran sulfate sodium-induced colitis in mice," *Food & Function*, vol. 11, no. 1, pp. 846–859, 2020.

[46] C. Tan, M. Wang, Y. Kong et al., "Anti-inflammatory and intestinal microbiota modulation properties of high hydrostatic pressure treated cyanidin-3-glucoside and blueberry pectin complexes on dextran sodium sulfate-induced ulcerative colitis mice," *Food & Function*, vol. 13, no. 8, pp. 4384–4398, 2022.

[47] X. Xiang, Q. Jiang, W. Shao et al., "Protective effects of shrimp peptide on dextran sulfate sodium-induced colitis in mice," *Frontiers in Nutrition*, vol. 8, Article ID 773064, 2021.

[48] J. F. Chen, D. D. Luo, Y. S. Lin et al., "Aqueous extract of Bruguiera gymnorrhiza leaves protects against dextran sulfate sodium induced ulcerative colitis in mice via suppressing NF-κB activation and modulating intestinal microbiota," *Journal of Ethnopharmacology*, vol. 251, Article ID 112554, 2020.

[49] J. D. Schulzke, S. Ploeger, M. Amasheh et al., "Epithelial tight junctions in intestinal inflammation," *Annals of the New York Academy of Sciences*, vol. 1165, no. 1, pp. 294–300, 2009.

[50] W. Huang, Z. Deng, L. Lu et al., "Polysaccharides from soybean residue fermented by neurospora crassa alleviate dss-induced gut barrier damage and microbiota disturbance in mice," *Food & Function*, vol. 13, no. 10, pp. 5739–5751, 2022.

[51] Y. Xu, H. Feng, Z. Zhang et al., "The protective role of scorias spongiosa polysaccharide-based microcapsules on intestinal barrier integrity in dss-induced colitis in mice," *Foods*, vol. 12, no. 3, p. 669, 2023.

[52] J. I. Grill, J. Neumann, F. Hiltwein, F. T. Kolligs, and M. R. Schneider, "Intestinal E-cadherin deficiency aggravates dextran sodium sulfate-induced colitis," *Digestive Diseases and Sciences*, vol. 60, no. 4, pp. 895–902, 2015.

[53] X. Xu, J. Wu, Y. Jin, K. Huang, Y. Zhang, and Z. Liang, "Both Saccharomyces boulardii and its postbiotics alleviate dextran sulfate sodium-induced colitis in mice, association with modulating inflammation and intestinal microbiota," *Nutrients*, vol. 15, no. 6, p. 1484, 2023.

[54] L. Li, N. Qiu, Y. Meng et al., "Preserved egg white alleviates dss-induced colitis in mice through the reduction of oxidative stress, modulation of infl ammatory cytokines, nf-κb, mapk and gut microbiota composition," *Food Science and Human Wellness*, vol. 12, no. 1, pp. 312–323, 2023.

[55] E. Zigmond, B. Bernshtein, G. Friedlander et al., "Macrophage-restricted interleukin-10 receptor deficiency, but not il-10 deficiency, causes severe spontaneous colitis," *Immunity*, vol. 40, no. 5, pp. 720–733, 2014.

[56] Y. Ren, Y. Geng, Y. Du et al., "Polysaccharide of hericium Erinaceus attenuates colitis in C57bl/6 mice via regulation of oxidative stress, inflammation-related signaling pathways and modulating the composition of the gut microbiota," *The Journal of Nutritional Biochemistry*, vol. 57, pp. 67–76, 2018.

[57] R. Zhang, S. Yuan, J. Ye et al., "Polysaccharide from flammuliana velutipes improves colitis via regulation of colonic microbial dysbiosis and inflammatory responses," *International Journal of Biological Macromolecules*, vol. 149, pp. 1252–1261, 2020.

[58] Y. Li, H. Ye, T. Wang et al., "Characterization of low molecular weight sulfate Ulva polysaccharide and its protective effect against ibd in mice," *Marine Drugs*, vol. 18, no. 10, p. 499, 2020.

[59] K. Wang, W. Li, K. Wang, B. Du, Z. Hu, and L. Zhao, "Litchi thaumatin-like protein induced the liver inflammation and altered the gut microbiota community structure in mice," *Food Research International*, vol. 161, Article ID 111868, 2022.

[60] X. Pan, M. Yin, M. Guo, X. Niu, and L. Han, "The latest progress of natural food polysaccharides preventing ulcerative colitis by regulating intestinal microbiota," *Journal of Functional Foods*, vol. 96, Article ID 105201, 2022.

[61] S. T. Miao, Q. S. Lu, Y. J. Zhou, Y. N. Chang, T. Xu, and M. Y. Zhu, "Oral administration of octacosanol modulates the gut bacteria and protects the intestinal barrier in ulcerative colitis mice," *Journal of Food Biochemistry*, vol. 46, no. 10, 2022.

[62] M. Shamoon, N. M. Martin, and C. L. O'Brien, "Recent advances in gut microbiota mediated therapeutic targets in inflammatory bowel diseases: emerging modalities for future pharmacological implications," *Pharmacological Research*, vol. 148, Article ID 104344, 2019.

[63] G. Huang, Z. Wang, G. Wu et al., "Lychee (litchi chinensis sonn.) pulp phenolics activate the short-chain fatty acid-free fatty acid receptor anti-inflammatory pathway by regulating microbiota and mitigate intestinal barrier damage in dextran sulfate sodium-induced colitis in mice," *Journal of Agricultural and Food Chemistry*, vol. 69, no. 11, pp. 3326–3339, 2021.

[64] R. Al-Sadi, V. Dharmaprakash, P. Nighot et al., "Bifidobacterium bifidum enhances the intestinal epithelial tight junction barrier and protects against intestinal inflammation by targeting the toll-like receptor-2 pathway in an NF-κB-

Independent manner," *International Journal of Molecular Sciences*, vol. 22, no. 15, p. 8070, 2021.

[65] Y. Zhao, H. Chen, W. Li et al., "Selenium-containing tea polysaccharides ameliorate dss-induced ulcerative colitis via enhancing the intestinal barrier and regulating the gut microbiota," *International Journal of Biological Macromolecules*, vol. 209, pp. 356–366, 2022.

[66] J. Mo, J. Ni, M. Zhang et al., "Mulberry anthocyanins ameliorate dss-induced ulcerative colitis by improving intestinal barrier function and modulating gut microbiota," *Antioxidants*, vol. 11, no. 9, p. 1674, 2022.